ISSN 2096-7071
CN 10-1629/R1

CHINA CDC WEEKLY

Vol. 4 No. 23 Jun. 10, 2022

CCDC weekly

中国疾病预防控制中心周报

COVID-19 ISSUE (27)

Preplanned Studies

SARS-CoV-2 Aerosol Transmission Through Vertical Sanitary Drains in High-Rise Buildings — Shenzhen, Guangdong Province, China, March 2022 489

An Analysis of Life-Year Lost Due to COVID-19 — 34 Countries, December 2019–March 2021 494

Commentary

Measuring the Effect of COVID-19 Pandemic on Mortality: Review and Prospect — China, 2021 499

Methods and Applications

Field Evaluation of a Duplex RT-RAA Assay for Rapid Detection of SARS-CoV-2 — Hebei Province, China, January 2021 504

Novaferon Effectively Inhibits Ancestral SARS-CoV-2 and Omicron Variant *in Vitro*, 2022 509

ISSN 2096-7071

China CDC Weekly

Cover photo: Dongqun Xu from China CDC explaining an areosol tansmission simulation experiment in a community with a SARS-CoV-2 cluster outbreak in Shenzhen, Guangdong Province, March 28, 2022.

Preplanned Studies

SARS-CoV-2 Aerosol Transmission Through Vertical Sanitary Drains in High-Rise Buildings — Shenzhen, Guangdong Province, China, March 2022

Keyang Lyu[1,&]; Siyang Feng[2,&]; Xia Li[1]; Qin Wang[1]; Xiaoning Zhao[3]; Shuyuan Yu[2]; Ping Zheng[1]; Jiajia Ji[2]; Guomin Chen[2]; Jing Liang[4]; Tao Lan[2]; Jinshu Feng[2]; Shuai Jiang[2]; Jianhua Lu[2]; Tianlong Xia[2]; Chaoqiong Peng[2]; Tiejian Feng[2,#]; Dongqun Xu[1,#]

Summary

What is already known about this topic?

Aerosol transmission of severe acute respiratory syndrome coronavirus 2 (SARS-CoV-2) via sanitary pipelines in high-rise buildings is possible, however, there is a lack of experimental evidence.

What is added by this report?

The field simulation experiment confirmed the existence of a vertical aerosol transmission pathway from toilet flush-soil stack-floor drains without water seal. This report provided experimental evidence for vertical aerosol transmission of clustered outbreaks on 18 floors of a 33-story residential building.

What are the implications for public health practice?

The water seal on floor drains is a necessary barrier to prevent the risk of vertical aerosol transmission of infectious disease pathogens in buildings. It is necessary not only to have a U-shaped trap in the drainage pipe, but also to be filled with water regularly.

In several epidemiological reports, clustered outbreaks of coronavirus disease 2019 (COVID-19) in residential buildings show vertical distribution (*1*–*2*). Some research suggested that the negative pressure caused by the exhaust fan in bathrooms or the stronger chimney effect during non-toilet flushing periods drives virus aerosols into soil stacks entering from the floor drains or pipe leaks (*2*–*4*). Another study, which excluded the effects of exhaust fans and assumed that toilet flushing-floor drains without water seal were the primary contributor to aerosolization lacked experimental evidence (*1*). In addition, the aerodynamic characteristics of tracer gases used in field simulation experiments cannot be used to make meaningful conclusions about aerosols (*5*). In our previous research the aerosol simulants were used to confirm the viral aerosols generated by toilet flushing in the sewage pipe. The results showed that under certain conditions, it caused cross-floor non-vertical aerosol transmission between 3 floors in a quarantined hotel (*6*).

A recent COVID-19 clustered outbreak occurred in a 33-story building in Shenzhen City, Guangdong Province in March 2022. In total, 62.9% (39/62) of the confirmed cases lived in a vertical building layout on 18 different floors (room 707, room 907, ... room 3007). According to the epidemiological investigation, those cases were not close contacts. Therefore, it is presumed that cross-floor vertical transmission of the viral aerosols occurred. The onsite investigation found that there were no U-shaped traps in the drainage pipe and the floor drains had no water seals in the building (Figure 1). Polystyrene fluorescent microspheres with similar aerodynamic characteristics to the severe acute respiratory syndrome coronavirus 2 (SARS-CoV-2) spike pseudovirus were used as simulants to explore the path of the viral aerosols in this building through field simulation experiments. The fluorescent microspheres were observed in samples from every site. This showed that there was a clear transmission path from toilet flush to soil stacks and floor drains without water seal in the high-rise building.

The COVID-19 outbreak in clusters in high-rise buildings through the path of toilet flush-soil stack-floor drains without water seal occurs. This experiment not only confirmed the vertical aerosol transmission pathway, but also had important public health significance for the prevention and control of COVID-19 in residential buildings, hotels, and other buildings, where the U-shaped trap must be designed in the drainage pipe. In addition, the floor drain should be regularly checked and filled with water to reduce the possibility of vertical aerosol transmission of infectious disease pathogens in buildings.

According to the daily habits of residents, combined

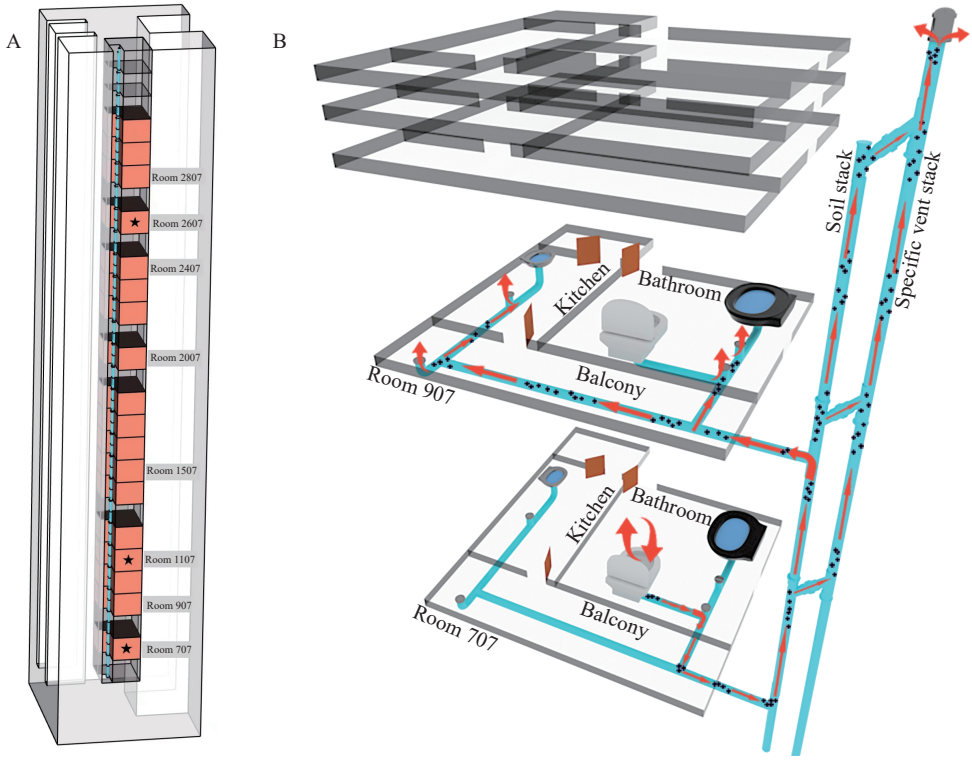

FIGURE 1. Diagram of positive case distribution and cross-layer vertical aerosol transmission of the 7th house layout in the high-rise building. (A) The diagram of the positive cases distributed in 7th house layout across 18 floors and rooms of field simulation experiment in the 33-story building. (B) The diagram of the drainage pipelines and soil stack system in the 7th house layout.

Notes: In the diagram of positive cases distributed in the building, the orange blocks indicate the rooms of confirmed positive cases in the 7th house layout, the black stars indicate the rooms of simulating defecation and toilet flushing (room 707 in scenario 1, rooms 707, 1107, and 2607 in scenario 2), and the sampling room are also noted with room numbers. In the diagram of drainage pipelines and soil stack systems, the black particles indicate the viral aerosol simulant generated by defecation and toilet flushing and the red arrows indicate the transmission pathway of the viral aerosols.

with the epidemiological investigation information, the time of detection of positive nucleic acid tests, and considering the neutral pressure plane and the Chimney Effect, the field simulation experiment was carried out with the bathroom window and exhaust fan closed. Two scenarios were designed using polystyrene fluorescent microspheres as the simulants. The method of preparation of simulants, as well as the sampling, field monitoring and laboratory analysis methods after toilet flushing were detailed in a previous research (*7*). Room 707, where the index patient lived, was selected to simulate defecation in the first scenario. Before patients in room 707 were transferred to the designated hospital, there was a risk of vertical aerosol transmission to the upper floors, so rooms 707, 1107, and 2607 were selected to simulate defecation in the second scenario. In the two scenarios, when the simulated bathroom toilet flushed, the rest of other bathrooms' toilets flushed at the same time with different arrangements of the combination (Supplementary Table S1, available in https://weekly.chinacdc.cn/).

The change of wind speed of floor drain, take room 707 as an example, the wind speed of the floor drains varied with the number of toilet flushing, and the peak value was prolonged with an increase in the number of toilet flushing. Except for room 1507, which was located on the neutral pressure plane, the wind speed of the floor drains in all other rooms changed (Supplementary Figure S1, available in https://weekly.chinacdc.cn/).

As the number of toilet flushing increased along with the extension of the simulation time, the number of small particle-size aerosols trended upward, with a few exceptions. Within the same room, the trend of different particle sizes was relatively the same at different times (Supplementary Figure S2, available in https://weekly.chinacdc.cn/). The trend of large particle-size aerosols had no obvious regularity which had fewer total particles and were easily affected by

various factors.

Except for the first scenario in room 1507, the fluorescent microspheres were observed in all filter membrane samples. The fluorescent microspheres were also observed on smear swab samples from the floor drains of the kitchens except room 1507. No smear swab samples were collected from the kitchen of rooms 1107 and 2607 because the floor drains were hidden in the cupboards. In addition, the fluorescent microspheres were observed on the smear swab samples from the bathroom floor drain in room 1507 in the second scenario (Table 1, Figure 2).

DISCUSSION

In our research at a quarantined hotel, the stack exhaust channel was arbitrarily changed. The viral aerosols generated by toilet flushing in the sewage pipe could not be discharged from the exhaust port, and therefore entered the cross-floor vertical units through the floor drains without water seal (*6*). The aerosols in the bathroom entered via the exhaust fan connected to the exhaust air shaft. This pushed aerosols across vertical units of the hotel, across the floor under specific meteorological conditions, resulting in vertical transmission across the 5th through 7th floor. In addition, the hotel rooms adopted a mix of fresh air and recycled air, resulting in non-vertical transmission on the same floor. The combination of the above three effects resulted in the cross-floor non-vertical aerosol transmission of SARS-CoV-2. However, this outbreak occurred in clusters on 18 floors with the 7th vertical house layout (Figure 1). The bathroom exhaust fan and windows of this unit face the balcony and were connected to the kitchen. The windows of balcony remained open at all times. No matter whether the bathroom exhaust fan or the kitchen ventilator were turned on, negative pressure could not be formed. Therefore, the exhaust fans and the kitchen ventilators were not opened during the simulation. Flushing the

TABLE 1. The observation results of fluorescent microspheres of filter membrane sample and smear swab sample.

No. of rooms	Scenario 1	Scenario 2	
	Filter membrane sample	Filter membrane sample	Smear swab sample
907	●	●	●
1107	●	●	
1507	●	●	
2007	●	●	●
2407	●	●	●
2607	●	●	
2807	●	●	●

Note: The aerosol filter membrane samples collected by medium flow PM_{10} samplers (100 L/min) in the bathroom of each room. The smear swab samples were collected from the floor drain of the kitchen by cotton swab. No smear swab samples were collected from the kitchen of rooms 1107 and 2607 because the floor drains were hidden in the cupboards. The smear swab samples of room 1507 were not observed. The green dots (●) showed where simulants were observed in samples.

FIGURE 2. Representative photos of fluorescent microspheres tracked by different sampling methods at different rooms in 2 scenarios. (A) the aerosol filter membrane sample of room 2807 during scenario 1; (B) the aerosol filter membrane sample of room 1107 during scenario 2; (C) smear swab sample from the floor drain of the kitchen of room 1107 during scenario 2.
Note: After simulating defecation and toilet flushing, fluorescent microspheres (green) were observed using fluorescent microscopy.

toilet in other vertical units directly affected the wind speed of the floor drain in room 707, while the wind speed of the floor drains in room 1507 had no significant change. The wind speed in the floor drain could partly indicate the pressure changes during toilet flushing. Similar pressure changes due to flushing were shown in previous studies (*8*), while the neutral pressure plane held a relatively stable pressure. The sewage and waste water of the bathroom, kitchen, and balcony were gathered and discharged into a dual-stack system in this building. There were no U-shaped traps in the drainage pipes in the building nor floor drains with water seal in the bathroom, kitchen, or balcony. The washing machine drain pipe plugs into the floor drain on the balcony. With the exhaust fans turned off, even in scenario 1 where the simulants were only poured into the toilet of room 707, after toilet flushing, the fluorescent microspheres could be observed on all the filter membrane samples from the bathroom. That confirmed the existence of a vertical aerosol transmission path from the toilet flush-soil stack-floor drain without water seal and provided experimental evidence for the outbreak in clusters across floors within high-rise buildings.

It is very common that toilets are used and flushed at the same time on different floors in high-rise buildings. When COVID-19 patients use toilets, they excrete virus. The simultaneous use of toilets on multiple floors exacerbated the spread of viral aerosols through the path of toilet flush-soil stack-floor drain without water seal. Although the neutral pressure plane was located on the 15th floor, when the toilet was flushed, the wind speed of the floor drain changed slightly. The pressure balance in it broke with the increase in the number of toilets being flushed simultaneously. The simulants were also observed on the filter membrane sample and smear swab sample from the bathroom of room 1507 in scenario 2, therefore the spread path also existed in the neutral pressure plane. The viral aerosol generated by toilet flushing in the soil stack would therefore spread into rooms from the floor drain without water seal.

This study was subject to some limitations. The field simulation experiment was a qualitative study. The experimentally confirmed aerosol transmission of the simulant does not represent the risk of infection posed by the virus.

The field simulation experiment showed the existing path of the toilet flush-soil stack-floor drain without water seal and its risks in high-rise buildings without U-shaped traps and water seal. Therefore, property management companies should check traps and water seal. Where it is possible odor-proof floor drains should be added into older buildings. Meanwhile, health education should be strengthened to teach building residents how to fill their floor drains regularly to ensure the water seal is deep enough (≥50 mm) in order to cut off the aerosol transmission. In addition, if bathrooms have windows facing the outside, the windows should be opened frequently for ventilation. If not, an exhaust fan needs to be installed and turned on frequently for ventilation in the case of ensuring that the floor drain water seal is deep enough. If the condition of water seal is uncertain, the bathroom door should first be opened, and then the exhaust fan should be turned on for ventilation. During the pandemic, if there are positive cases in the same house layout within a building, the chlorine-containing disinfectants can be poured into the floor drain regularly to effectively kill the virus.

Conflicts of Interest: No conflicts of interest.

Acknowledgments: Other experts from Shenzhen Center for Disease Control and Prevention and Futian District Center for Disease Control and Prevention.

Funding: Supported by the Key Program of National Natural Science Foundation of China (92043201).

doi: 10.46234/ccdcw2022.108

[#] Corresponding authors: Tiejian Feng, fengtiej@126.com; Dongqun Xu, xudq@chinacdc.cn.

[1] Key Laboratory of Environment and Population Health, National Institute of Environmental Health, Chinese Center for Disease Control and Prevention, Beijing, China; [2] Shenzhen Center for Disease Control and Prevention, Shenzhen City, Guangdong Province, China; [3] Division of Chemical Analysis, Biology and Medicine, Beijing Institute of Metrology, Beijing, China; [4] Futian District Center for Disease Control and Prevention, Shenzhen City, Guangdong Province, China.

[&] Joint first authors.

Submitted: May 05, 2022; Accepted: June 08, 2022

REFERENCES

1. Han T, Park H, Jeong Y, Lee J, Shon E, Park MS, et al. COVID-19 cluster linked to aerosol transmission of SARS-CoV-2 via floor drains. J Infect Dis 2022;225(9):1554 – 60. http://dx.doi.org/10.1093/infdis/jiab598.
2. Wang Q, Li YG, Lung DC, Chan PT, Dung CH, Jia W, et al. Aerosol transmission of SARS-CoV-2 due to the chimney effect in two high-rise housing drainage stacks. J Hazard Mater 2022;421:126799. http://dx.doi.org/10.1016/j.jhazmat.2021.126799.
3. Hung LS. The SARS epidemic in Hong Kong: What lessons have we learned? J Roy Soc Med 2003;96(8):374 – 8. http://dx.doi.org/10.1258/jrsm.96.8.374.
4. Kang M, Wei JJ, Yuan J, Guo JX, Zhang YT, Hang J, et al. Probable

evidence of fecal aerosol transmission of SARS-CoV-2 in a high-rise building. Ann Intern Med 2020;173(12):974 – 80. http://dx.doi.org/10.7326/M20-0928.
5. Wang Q, Lin Z, Niu JL, Choi CKY, Fung JCH, Lau AKH, et al. Spread of SARS-CoV-2 aerosols via two connected drainage stacks in a high-rise housing outbreak of COVID-19. J Hazard Mater 2022;430:128475. http://dx.doi.org/10.1016/j.jhazmat.2022.128475.
6. Zhang ZN, Li X, Wang Q, Zhao XN, Xu J, Jiang QQ, et al. Simulation studies provide evidence of aerosol transmission of SARS-CoV-2 in a multi-story building via air supply, exhaust and sanitary pipelines. Int J Environ Res Public Health 2022;19(3):1532. http://dx.doi.org/10.3390/ijerph19031532.
7. Zhang ZN, Li X, Wang Q, Xu J, Jiang QQ, Lyu J, et al. Field simulation of aerosol transmission of SARS-CoV-2 in a special building layout—Guangdong Province, China, 2021. China CDC Wkly 2021;3(34):711 – 5. http://dx.doi.org/10.46234/ccdcw2021.176.
8. Jo JH, Seok HT, Yeo MS, Kim KW. Simplified prediction method of stack-induced pressure distribution in high-rise residential buildings. J Asian Archit Build Eng 2009;8(1):283 – 90. http://dx.doi.org/10.3130/jaabe.8.283.

SUPPLEMENTARY MATERIALS

SUPPLEMENTARY TABLE S1. The array and combination mode of defection simulation and toilet flushing in 2 scenarios.

Scenario	Time (min)	Room numbers							
		707	907	1107	1507	2007	2407	2607	2807
1	10	D/F	F						F
	20	D/F		F			F		
	30	D/F		F				F	F
	40	D/F	F		F		F		
	50	F		F		F		F	F
	60	F	F		F	F	F		
2	10	D/F	F	D/F				D/F	F
	20	D/F		D/F	F		F	D/F	
	30	D/F	F	D/F	F			D/F	F
	40	D/F	F	D/F		F	F	D/F	
	50	F	F	F	F		F	F	F
	60	F	F	F		F	F	F	F

Note: The simulants were poured into the toilet for the first 40 minutes of the simulation experiment, and the toilet was flushed every 10 minutes. The letter “D” means pouring simulants into the toilet, and letter “F” indicates toilet flushing.

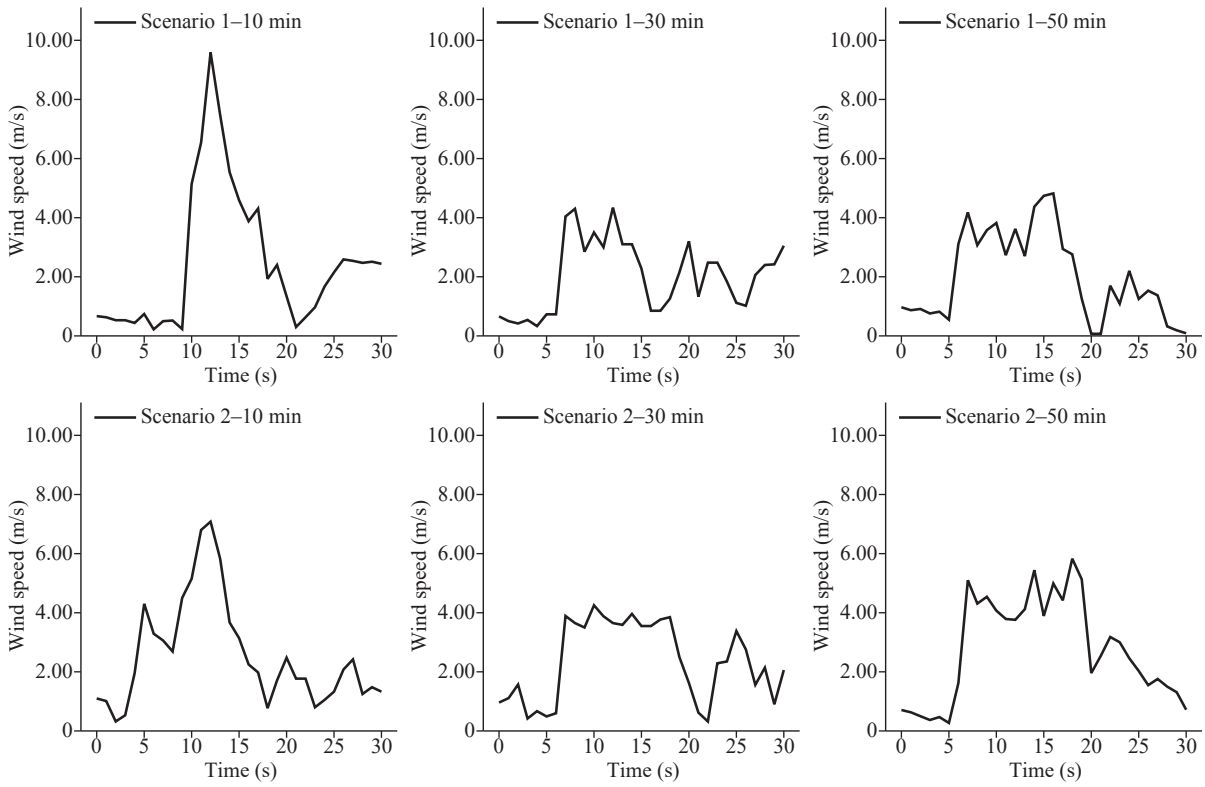

SUPPLEMENTARY FIGURE S1. Representative variations of the wind speed in the bathroom floor drain of room 707 during 2 scenarios.

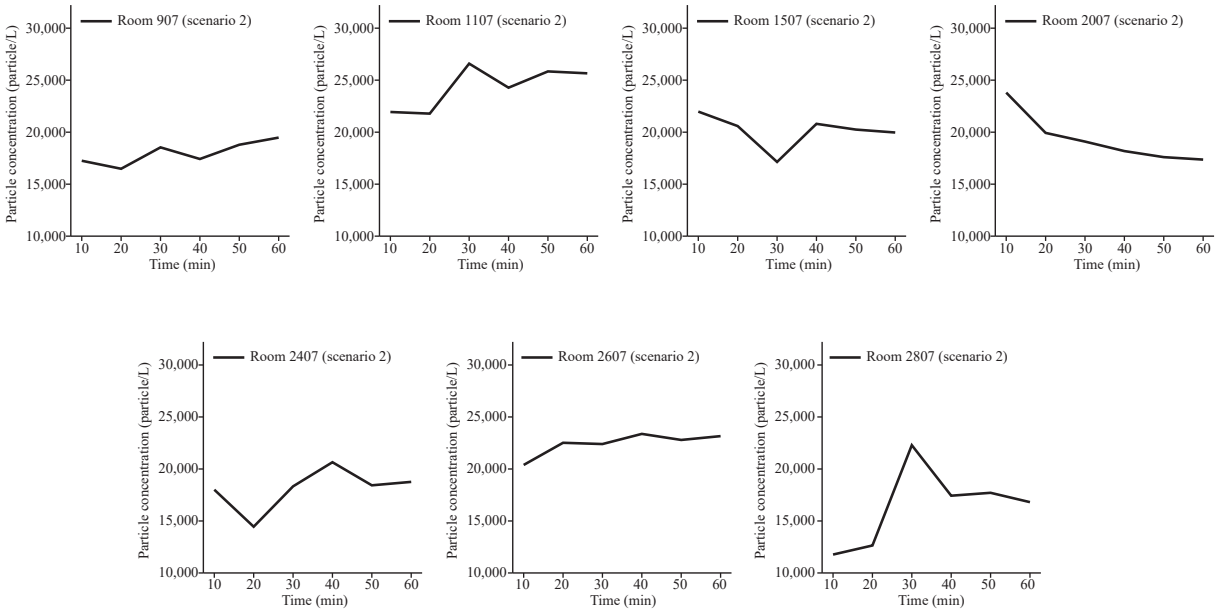

SUPPLEMENTARY FIGURE S2. The changes of particle concentration over time at 0.3 μm in scenario 2 at different rooms.

Preplanned Studies

An Analysis of Life-Year Lost Due to COVID-19 — 34 Countries, December 2019–March 2021

Shan Jiang[1,&]; Dan Cai[2,&]; Daqin Chen[2]; Yawen Jiang[2,#]

Summary

What is already known about this topic?

The coronavirus disease 2019 (COVID-19) pandemic has caused severe health consequences. Though most COVID-19 deaths occurred among very old people, their life-year loss might be very large because of their life expectancy at that age.

What is added by this report?

This study quantified how many years of life were lost due to COVID-19 in 34 countries. COVID-19 caused 9 to 21 years of life lost (YLL) per deceased patient. East Asia and Oceania had substantially lower per capita YLL than North America and Europe. Among all countries included, the United States had the greatest total YLL, Peru had the largest YLL per 100,000 people, and Mexico had the largest YLL per 100,000 COVID-19 patients.

What are the implications for public health practice?

The YLL quantification indicated that the vulnerable population, especially the elderly, should be protected under careful public health measures to reduce their YLL. It also implied that it might be too early to lift anti-epidemic restrictions now, since the extreme disproportionate consequences (total and per-capita YLL) in different countries underscored the scrutinization over the variation in disease control strategies to optimize future disease control and prevention.

The coronavirus disease 2019 (COVID-19) pandemic has caused severe health consequences. This study aimed to estimate the years of life lost (YLL) associated with COVID-19 in different countries. We collected data on COVID-19 cases and deaths up to March 27, 2021 and used a method recommended by the World Health Organization (WHO) to calculate YLL. We assessed the total YLL of each included country and calculated the YLL per 100,000 patients and per 100,000 people. We included 34 countries in the analysis. The US had the greatest total YLL among all countries. Peru topped the per-capita YLL. Mexico suffered from the greatest YLL per 100,000 patients. COVID-19 caused 9 to 21 YLL per deceased patient. East Asia and Oceania had substantially lower per capita YLL than North America and Europe. The pandemic caused disproportionate consequences (total and per-capita YLL) in different countries, implying that the variation in disease control strategies should be scrutinized to optimize future disease control and prevention.

As of November 2021, over 255 million COVID-19 cases were confirmed globally, almost 3 million of whom lost their lives (*1*). The spread of the virus remains fast. While numerous studies have provided insights into COVID-19-related mortality, very few emphasized the life expectancies and life-year loss of the deceased. Some argued that the majority of COVID-19 deaths occurred among the "oldest-old" who were proximal to death even without COVID-19 (*2*). However, the life-year loss of such individuals might be large given their life expectancy at that age (*3*). Estimating the COVID-19-related life-year loss is important to understand the societal loss and to inform the choice of epidemic containment strategies. YLL, an established measure to assess the impact of premature death, captures the additional time a patient would have lived if the patient did not die prematurely (*4*). It refers to the difference between the age of death and the life expectancy at that age. Compared with crude mortality and the number of deaths, YLL aims to comprehensively measure the disease burden. There is an absence of cross-country comparison to provide a worldwide landscape of YLL due to COVID-19 (*5*). This study aimed to provide YLL information for the debate and reflection on the anti-epidemic strategies and the establishment of a comprehensive loss function of COVID-19.

We categorized the COVID-19 patients and population into 9 age groups. The calculation of YLL followed the recommendation by the World Health Organization (Supplementary Materials, available in https://weekly.chinacdc.cn/). Accordingly, we

calculated the primary outcomes, including YLL per 100,000 COVID-19 patients and per 100,000 people. Standard errors were estimated using Monte Carlo simulation with 1,000 repetitions (ndard errors were estimated using Monte Carlo simulation with 1,000 repetitions (*6*–*7*). We assumed that the death events were uniformly distributed within each age group, so that we were able to approximate the YLL of each group by multiplying the number of deaths and the life expectancy of the median age of the group (e.g., the life expectancy of age 4.5 represented the mean life expectancy of group 0–9). We collected data of the life expectancy of different ages, demographic data of different countries, COVID-19 cases, deaths, and their age distributions (Supplementary Table S1 available in https://weekly.chinacdc.cn/). We included countries with age-specific data available on the incidence and mortality of COVID-19 as of March 2021. Two analysts collected data independently and cross-checked the data. We used Excel 2016 (Microsoft Corporation, United States, North America) and Crystal Ball (version 11.1.1, Oracle Corporation, United States, North America) for analysis and Monte Carlo simulation.

We developed some secondary outcomes using primary outcomes. By dividing YLL per 100,000 patients and deaths per 100,000 patients, we derived YLL per dead patient, indicating the average YLL for every death caused by COVID-19. The 95% credible interval of YLL per dead patient was calculated by simulating the numerator and denominator simultaneously using Monte Carlo simulation 1,000 times. Moreover, by combining the results of countries in the same continental region, we compared the outcomes in five regions: East Asia, Southeast Asia, Europe, North America, and Oceania.

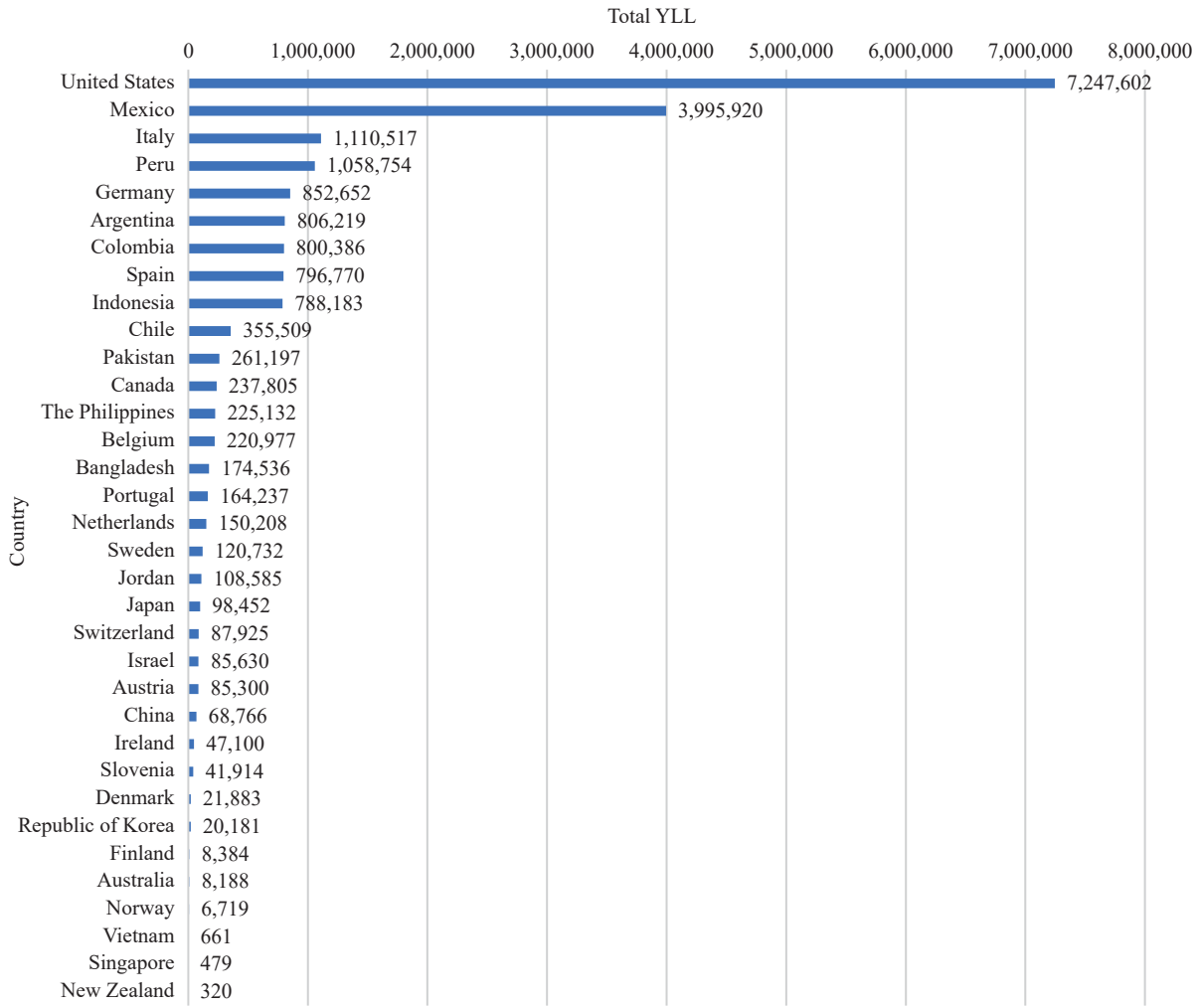

FIGURE 1. Total years of life lost caused by COVID-19 by country.
Note: Countries are sorted in an order of decreasing YLL per 100,000 people.

Among the 34 included countries, the total YLL in the US (7.2 million) was substantially greater than in other countries, almost twice as much as in Mexico (3.99 million). Italy, Peru, Germany, Argentina, Colombia, Spain, and Indonesia had around 1 million YLL. Other countries included had less than 0.36 million. Vietnam, Singapore, and New Zealand had less than 1,000 YLL (Figure 1).

Figure 2 presented the cases, deaths, and YLL for every 100,000 people, in which countries were sorted in an order of decreasing YLL numbers. Peru, Mexico, and the US ranked in the top three in terms of YLL per 100,000 people. Although Peru and Mexico had much fewer per-capita cases than the US, they had similar COVID-19-relevant death rates, leading to a great loss of life years.

Countries with high case and death rates per 100,000 people usually had a greater loss of life years per 100,000 people, compared with those with low case and death rates; and vice versa (Supplementary Table S2, available in https://weekly.chinacdc.cn/). For example, Slovenia ranked top in terms of COVID-19 cases and deaths per 100,000 people and ranked fourth in per-capita YLL. Belgium ranked second in terms of deaths per 100,000 people and ranked fifth in per-capita YLL. As the first country reporting COVID-19, China's infection and death rates and YLL per capita were among the lowest in the countries included in the analysis.

Some exceptions existed. Although Israel ranked second in terms of infection rate, the death rate was low (71.2 per 100,000 people), leading to a moderate per-capita YLL (989.3). Among countries with lower than 100 YLL per capita, Singapore had a per-capita YLL as low as 8.2, despite that the infection rate in the country was higher than in other countries of this group. This might be because of its low mortality rate among the confirmed cases.

Figure 3 illustrated the YLL by continental region, in which the circle size was indicated by YLL per 100,000 people. With a much more population than other regions, East Asia had a low total YLL, leading to the lowest YLL per 100,000 people. In contrast, North America had the largest total YLL, though its population size was much smaller than that of East Asia. East Asian and Oceanic countries endured the smallest YLL for every 100,000 people (<30).

Supplementary Figure S1 (available in https://weekly.chinacdc.cn/) illustrated the results of YLL for every 100,000 COVID-19 patients by country. Mexico ranked first on both indicators. As the first country to report COVID-19, China ranked second and had a higher mortality rate and YLL per 100,000 patients than other countries except for Mexico. The US had a moderate death rate and YLL per 100,000 patients. The European countries had YLL ranging from 7,000 to 32,000 for every 100,000 patients. Italy had the highest YLL per 100,000 patients in Europe (31,833), while Norway had the lowest (7,389). Singapore had the least deaths and the lowest YLL per 100,000 patients among all countries. Generally, developing countries had a higher death rate and a higher per-patient YLL than developed countries. Supplementary Table S3 (available in https://weekly.chinacdc.cn/) demonstrated that the deceased patients lost 9 to 21 years of life on average across countries. Australia had the lowest per-patient YLL (9.008), while Peru had the highest per-patient YLL (20.75).

DISCUSSION

This analysis provided a landscape of COVID-19-related YLL accumulated from the start of the pandemic to March 2021 in 34 countries based on age-specific life expectancy. North America had a greater amount of YLL than other regions, and the US ranked first in terms of total YLL among the countries. East Asian and Oceanic countries had a lower per-capita YLL than other countries. The pandemic had caused 9 to 21 years of life lost for every deceased patient on average.

The YLL per deceased patient reminds us how life-threatening this disease could be. We call attention to the fact that COVID-19 patients may die long before their "time," although the crude mortality does not seem as scary as many other fatal diseases. It may be better to shield the vulnerable population, including the elderly and people with underlying diseases, instead of treating them carelessly (*8*).

It was reported that China, Republic of Korea, Norway, and Germany responded relatively faster than other countries since their respective first reported death cases and took a short time to enforce social distancing and contact tracing nationwide (*9*). In contrast, Spain responded relatively slowly to the initial outbreak, whereas Sweden did not take strict measures to limit the transmission (*9*). We observed that East Asian countries, Norway, and Germany had lower YLL per 100,000 people than those with slow response and/or lax measures, such as Spain. The YLL comparison may underline the importance of future research on quick response to COVID-19 and its health burden such as YLL, which may contribute to the consensus on appropriate anti-pandemic strategies.

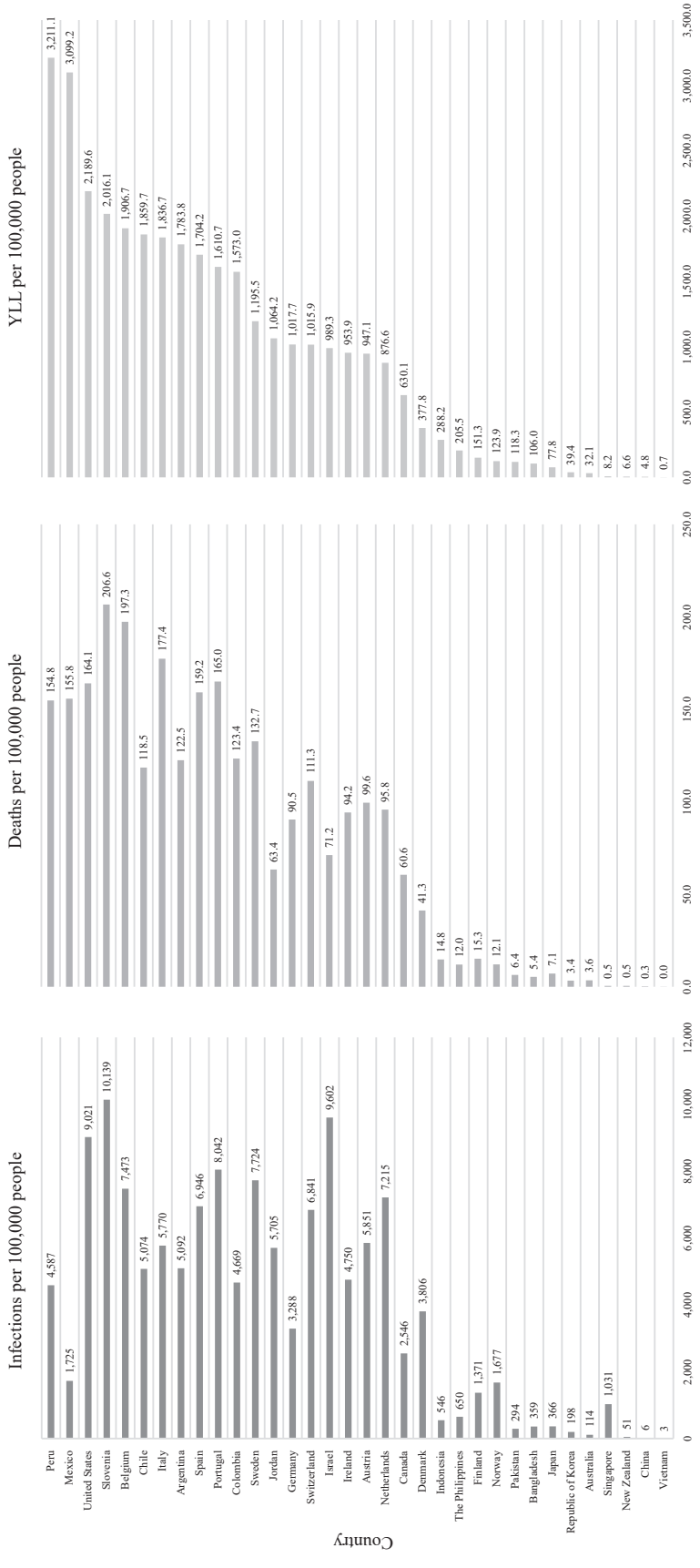

FIGURE 2. COVID-19 cases, deaths and years of life lost (YLL) for every 100,000 people by country.
Note: Countries are sorted in an order of decreasing YLL per 100,000 people.

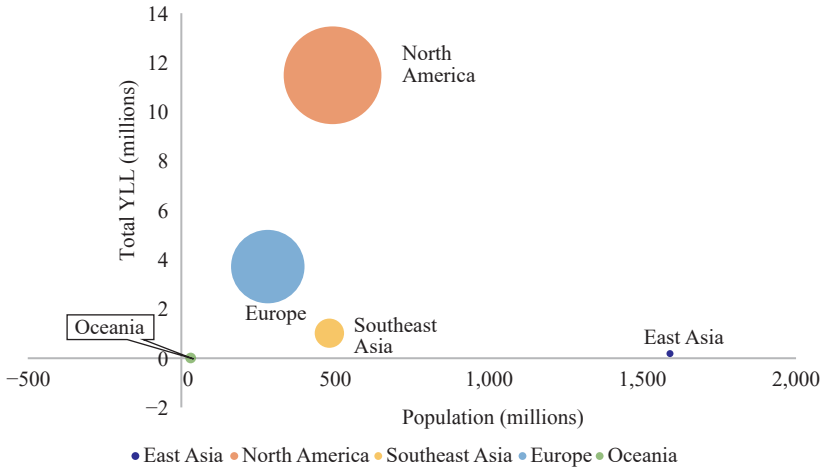

FIGURE 3. Total years of life lost (YLL) due to COVID-19 in some continental regions.

The pandemic continues and the virus keeps mutating. The current predominant pandemic in many countries is caused by the Delta and Omicron variants of coronavirus, which have greater transmissibility than previous variants. Many governments chose to reopen their countries to alleviate the negative impact on the economy of the pandemic. According to the YLL comparison and previous experience (*10*), it might be too early to lift anti-epidemic restrictions, especially when evidence indicates that vaccination and medication may significantly change the landscape of YLL and save lives (*11–12*).

The findings of the present analysis should be interpreted with several caveats, including potential underreporting or misclassification of COVID-19 deaths, the heterogeneous data reporting routines across countries, and the exclusion of many countries due to the absence of key data components. Future research should improve data quality and the scope of analyses.

The pandemic caused different total and per-capita life-year losses in different countries. The variation in disease control strategies underlying such disproportionate consequences should be scrutinized to optimize future efforts in disease control and prevention.

doi: 10.46234/ccdcw2022.109

[#] Corresponding author: Yawen Jiang, jiangyw26@mail.sysu.edu.cn.

[1] School of Population and Public Health, University of British Columbia, Vancouver, BC, Canada; [2] School of Public Health (Shenzhen), Sun Yat-sen University, Shenzhen City, Guangdong Province, China.
[&] Joint first authors.

Submitted: November 25, 2021; Accepted: May 31, 2022

REFERENCES

1. World Health Organization. Coronavirus disease (COVID-2019) situation reports. 2022. https://www.who.int/emergencies/diseases/novel-coronavirus-2019/situation-reports. [2021-10-31].
2. Banerjee A, Pasea L, Harris S, Gonzalez-Izquierdo A, Torralbo A, Shallcross L, et al. Estimating excess 1-year mortality from COVID-19 according to underlying conditions and age in England: a rapid analysis using NHS health records in 3.8 million adults. medRxiv, 2020. http://dx.doi.org/10.1101/2020.03.22.20040287.
3. Chan MS, van den Hout A, Pujades-Rodriguez M, Jones MM, Matthews FE, Jagger C, et al. Socio-economic inequalities in life expectancy of older adults with and without multimorbidity: a record linkage study of 1. 1 million people in England. Int J Epidemiol 2019;48(4):1340 – 51. http://dx.doi.org/10.1093/ije/dyz052.
4. Gardner JW, Sanborn JS. Years of potential life lost (YPLL)—what does it measure? Epidemiology 1990;1(4):322 – 9. http://dx.doi.org/10.1097/00001648-199007000-00012.
5. Hanlon P, Chadwick F, Shah A, Wood R, Minton J, McCartney G, et al. COVID-19–exploring the implications of long-term condition type and extent of multimorbidity on years of life lost: a modelling study. Wellcome Open Res 2021;5:75. http://dx.doi.org/10.12688/wellcomeopenres.15849.3.
6. Moran PAP. The estimation of standard errors in monte carlo simulation experiments. Biometrika 1975;62(1):1 – 4. http://dx.doi.org/10.1093/biomet/62.1.1.
7. Chiang CL. The life table and its applications. Malabar: Robert E. Krieger Publishing Company. 1984. https://openlibrary.org/books/OL3500112M/The_life_table_and_its_applications.
8. Chen SQ, Jones LA, Jiang S, Jin HJ, Dong D, Chen X, et al. Difficulty and help with activities of daily living among older adults living alone during the COVID-19 pandemic: a multi-country population-based study. BMC Geriatr 2022;22(1):181. http://dx.doi.org/10.1186/s12877-022-02799-w.
9. Hale T, Angrist N, Boby T, Cameron-Blake E, Hallas L, Kira B, et al. Variation in government responses to COVID-19. Blavatnik School of Government Working Paper. 2020. https://www.bsg.ox.ac.uk/sites/default/files/2020-12/BSG-WP-2020-032-v10.pdf. [2021-10-31].
10. Jiang YW, Cai D, Chen DQ, Jiang S. The cost-effectiveness of conducting three versus two reverse transcription-polymerase chain reaction tests for diagnosing and discharging people with COVID-19: evidence from the epidemic in Wuhan, China. BMJ Glob Health 2020;5(7):e002690. http://dx.doi.org/10.1136/bmjgh-2020-002690.
11. Jiang YW, Cai D, Chen DQ, Jiang S, Si L, Wu J. Economic evaluation of remdesivir for the treatment of severe COVID-19 patients in China under different scenarios. Br J Clin Pharmacol 2021;87(11):4386 – 96. http://dx.doi.org/10.1111/bcp.14860.
12. Jiang YW, Chen DQ, Cai D, Yi Y, Jiang S. Effectiveness of remdesivir for the treatment of hospitalized COVID-19 persons: a network meta-analysis. J Med Virol 2021;93(2):1171 – 4. http://dx.doi.org/10.1002/jmv.26443.

Supplementary Materials

The COVID-19 patients and population into 9 age groups were categorized (i.e., 0–9, 10–19, 20–29, 30–39, 40–49, 50–59, 60–69, 70–79, and 80 and above). The calculation of YLL followed the recommendation by the World Health Organization (WHO):

$$YLL = \sum_{i=1}^{n} (D_i \times L_i) \quad (1)$$

where n denotes the number of age groups, D_i is the number of deaths due to COVID-19 in age group i, and L_i is the life expectancy of age group i.

According to equation 1 and the age groups we defined, we developed the calculation of YLL per 100,000 COVID-19 patients and per 100,000 people as follows:

$$YLL\ per\ 100,000\ patients = \sum_{i=1}^{9} (p_i \times 100,000 \times \mu_i \times L_i) \quad (2)$$

$$YLL\ per\ 100,000\ people = \sum_{i=1}^{9} (P_i \times 100,000 \times \mu_i \times L_i) \quad (3)$$

where μ_i denotes the mortality rate in age group i due to COVID-19; p_i denotes the proportion of COVID-19 patients in age group i among patients of all age groups; P_i denotes the probability of COVID-19 cases in age group i, which was calculated as the quotient of the number of cases and the number of people in group i. Standard errors were estimated using Monte Carlo simulation with 1,000 repetitions (*1–2*).

We assumed that the death events were uniformly distributed within each age group, so that we were able to approximate the YLL of each group by multiplying the number of deaths and the life expectancy of the median age of the group (e.g., the life expectancy of age 4.5 represented the mean life expectancy of group 0–9). The life expectancy of different ages was from the WHO country-specific lifetables (*3*). The demographic data of different countries were from the United Nations World Population Prospects in 2019 (*4*). We collected data on COVID-19 cases, deaths, and their age distributions from January 1, 2020 to March 27, 2021, using data from WHO and corresponding countries and regions (*5–7*). We used Microsoft Excel 2016 (Microsoft Corporation, United States, North America) and Oracle Crystal Ball (version 11.1.1 Oracle Corporation, United States, North America) for analysis and Monte Carlo simulation.

We included countries with age-specific data available on the incidence and mortality of COVID-19 as of March 2021. When the data on the age distribution of COVID-19 cases and deaths exactly as of March 27, 2021, were not available, the information with the closest time stamp was carried forward. Due to the lack of information, the age distributions of confirmed cases in the UK were imputed using the pooled data of England and Scotland. When the age groups of the source data in a certain country were not defined coherently with the present analysis, they were mapped to the age groups defined in the present study by assuming a uniform distribution of cases within each age group in the source data. Data on the age distribution of the general population and the life expectancy of included countries were retrieved from PopulationPyramid.net, government websites, and WHO (*1–2*). Two analysts collected the data independently and cross-checked the data.

We developed secondary outcomes using primary outcomes such as deaths, YLL per 100,000 people, and YLL per 100,000 patients. By dividing YLL per 100,000 patients and deaths per 100,000 patients, we derived YLL per dead patient, indicating the average YLL for every death caused by COVID-19. The 95% confidence interval of YLL per dead patient was calculated by simulating the numerator and denominator simultaneously using Monte Carlo simulation 1,000 times. Moreover, we categorized the countries into eight regions: East Asia, Southeast Asia, South Asia, West Asia, Europe, North America, South America, and Oceania. We derived regional YLL outcomes by combining the results of countries in the same region. We extracted the data on COVID-19 cases and deaths from the sources listed Supplementary Table S1.

SUPPLEMENTARY TABLE S1. Data sources for COVID-19 cases and deaths in different countries.

Country/Region	Diagnosis	Death	Data reference
China	90,167	4,636	(*8*,*9*)
Italy	3,488,619	107,256	(*10*)
Republic of Korea	101,757	1,722	(*11*)
Spain	3,247,738	74,420	(*12*)
Germany	2,755,225	75,780	(*13*)

TABLE S1. (Continued)

Country/Region	Diagnosis	Death	Data reference
United States	29,859,706	543,003	(*14*,*15*)
Sweden	780,018	13,402	(*16*)
Norway	90,934	656	(*17*)
Australia	29,071	909	(*18*)
Canada	961,083	22,852	(*19*)
Singapore	60,288	30	(*20*,*21*)
Denmark	220,459	2,391	(*22*)
Japan	462,459	9,028	(*23*)
Portugal	820,042	16,827	(*22*)
Netherlands	1,236,209	16,421	(*24*)
Switzerland	592,090	9,631	(*25*)
Mexico	2,224,261	200,862	(*22*)
Vietnam	2,590	35	(*22*)
The Philippines	712,442	13,159	(*22*)
Bangladesh	591,214	8,878	(*22*)
Indonesia	1,494,589	40,449	(*22*)
Belgium	866,063	22,870	(*26*)
Austria	526,948	8,968	(*22*)
Chile	969,913	22,653	(*22*)
Peru	1,512,384	51,032	(*22*)
Israel	649,824	14,158	(*27*)
Finland	831,084	6,165	(*22*)
Pakistan	75,973	845	(*22*)
Argentina	2,375,591	62,790	(*22*)
Colombia	2,301,389	55,368	(*22*)
Jordan	582,133	6,472	(*22*)
Ireland	234,556	4,653	(*28*)
New Zealand	2,482	26	(*29*)
Slovenia	210,787	4,296	(*30*)

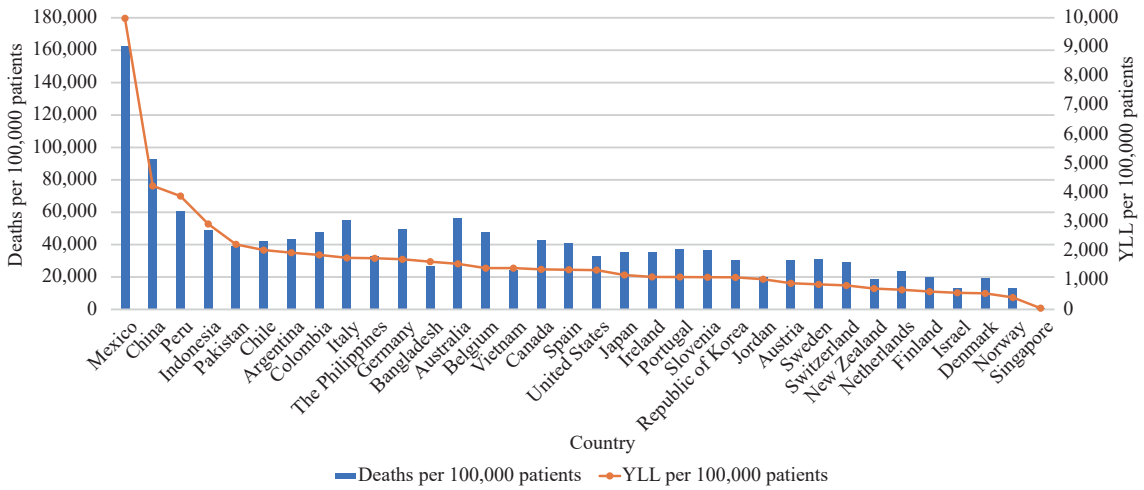

SUPPLEMENTARY FIGURE S1. Deaths and years of life lost for every 100,000 COVID patients.

SUPPLEMENTARY TABLE S2. COVID-19 cases, deaths, and years of life lost for every 100,000 people by country.

Country	Cases per 100,000 people	95% CI lower	95% CI upper	Deaths per 100,000 people	95% CI lower	95% CI upper	YLL per 100,000 people	95% CI lower	95% CI upper
Argentina	5,092	5,086	5,098	123	121	123	1,783.8	1,766.1	1,800.3
Australia	114	113	115	4	3	4	32.1	29.7	34.5
Austria	5,851	5,836	5,867	100	98	102	947.1	926.5	970.6
Bangladesh	359	358	360	5	5	5	106.0	103.4	108.2
Belgium	7,473	7,457	7,489	197	195	200	1,906.7	1,877.9	1,936.0
Canada	2,546	2,541	2,551	61	60	61	630.1	620.5	639.5
Chile	5,074	5,063	5,083	119	117	120	1,859.7	1,832.2	1,889.8
China	6	6	6	0	0	0	4.8	4.6	4.9
Colombia	4,669	4,663	4,675	123	122	124	1,573.0	1,556.9	1,588.2
Denmark	3,806	3,790	3,821	41	40	43	377.8	361.7	396.0
Finland	1,371	1,361	1,380	15	14	16	151.3	138.0	163.5
Germany	3,288	3,285	3,292	90	90	91	1,017.7	1,008.7	1,025.7
Indonesia	546	546	547	15	15	15	288.2	284.4	290.9
Ireland	4,750	4,731	4,769	94	91	97	953.9	917.3	989.8
Israel	9,602	9,581	9,620	71	70	73	989.3	960.5	1,018.8
Italy	5,770	5,764	5,776	177	176	178	1,836.7	1,824.1	1,850.2
Japan	366	365	367	7	7	7	77.8	76.1	79.6
Jordan	5,705	5,691	5,721	63	62	65	1,064.2	1,036.0	1,093.9
Mexico	1,725	1,723	1,727	156	155	156	3,099.2	3,083.4	3,114.2
Netherlands	7,215	7,202	7,227	96	94	97	876.6	862.0	893.1
New Zealand	51	49	54	1	0	1	6.6	3.7	9.5
Norway	1,677	1,667	1,688	12	11	13	123.9	112.7	135.7
Pakistan	294	293	295	6	6	7	118.3	115.4	120.0
Peru	4,587	4,581	4,596	155	154	156	3,211.1	3,181.2	3,243.4
The Philippines	650	649	652	12	12	12	205.5	201.1	209.6
Portugal	8,042	8,025	8,060	165	163	168	1,610.7	1,582.3	1,640.7
Singapore	1,031	1,023	1,038	1	0	1	8.2	4.7	11.6
Slovenia	10,139	10,099	10,180	207	201	213	2,016.1	1,942.6	2,086.2
Republic of Korea	198	197	200	3	3	4	39.4	36.9	41.3
Spain	6,946	6,939	6,953	159	158	160	1,704.2	1,690.2	1,718.6
Sweden	7,724	7,706	7,740	133	131	135	1,195.5	1,169.0	1,219.0
Switzerland	6,841	6,825	6,859	111	109	113	1,015.9	991.6	1,039.7
United States	9,021	9,018	9,024	164	164	164	2,189.6	2,182.7	2,196.3
Vietnam	3	3	3	0	0	0	0.7	0.4	0.9

Note: “Lower” means the lower bound of confidence interval (CI); “upper” means the upper bound of CI.
Abbreviations: 95% CI=95% confidence interval; YLL=years of life lost

SUPPLEMENTARY TABLE S3. Deaths and years of life lost per 100,000 COVID-19 patients by country and years of life lost per death caused by COVID.

Country	Deaths per 100,000 patients	95% CI lower	95% CI upper	YLL per 100,000 patients	95% CI lower	95% CI upper	YLL per death for patients	95% CI lower	95% CI upper
Argentina	2,406	2,387	2,425	35,032	34,688	35,383	14.56	14.41	14.71
Australia	3,127	2,956	3,305	28,166	26,239	30,047	9.01	8.32	9.65
Austria	1,702	1,670	1,734	16,188	15,813	16,559	9.51	9.26	9.76
Bangladesh	1,502	1,472	1,531	29,522	28,779	30,195	19.66	19.14	20.17
Belgium	2,641	2,609	2,672	25,515	25,131	25,897	9.66	9.50	9.80
Canada	2,378	2,349	2,406	24,743	24,397	25,123	10.41	10.25	10.57
Chile	2,336	2,309	2,362	36,654	36,063	37,211	15.69	15.45	15.95
China	5,142	5,014	5,277	76,266	73,865	78,905	14.83	14.31	15.41
Colombia	2,643	2,622	2,662	33,692	33,366	33,982	12.75	12.63	12.88
Denmark	1,085	1,045	1,125	9,926	9,482	10,390	9.15	8.69	9.62
Finland	1,112	1,043	1,180	11,036	10,148	11,888	9.92	9.15	10.80
Germany	2,750	2,733	2,768	30,947	30,723	31,201	11.25	11.15	11.35
Indonesia	2,706	2,678	2,732	52,736	52,086	53,265	19.49	19.23	19.73
Ireland	1,984	1,930	2,038	20,080	19,409	20,814	10.12	9.74	10.50
Israel	742	723	760	10,303	10,000	10,625	13.89	13.44	14.35
Italy	3,074	3,058	3,091	31,833	31,627	32,055	10.35	10.28	10.43
Japan	1,952	1,916	1,989	21,289	20,801	21,772	10.91	10.62	11.17
Jordan	1,112	1,088	1,140	18,653	18,129	19,221	16.78	16.23	17.30
Mexico	9,031	8,996	9,063	179,652	178,838	180,485	19.89	19.79	20.00
Netherlands	1,328	1,308	1,348	12,151	11,933	12,367	9.15	8.97	9.34
New Zealand	1,048	727	1,415	12,910	7,566	18,753	12.32	7.41	19.26
Norway	721	670	773	7,389	6,662	8,085	10.24	9.27	11.37
Pakistan	2,179	893	3,486	40,195	22,251	58,558	18.45	9.54	37.09
Peru	3,374	3,346	3,401	70,006	69,328	70,717	20.75	20.53	20.97
Philippines	1,847	1,817	1,879	31,600	30,924	32,281	17.11	16.71	17.51
Portugal	2,052	2,023	2,081	20,028	19,685	20,387	9.76	9.57	9.93
Singapore	50	32	66	795	457	1,109	15.97	9.99	24.23
Slovenia	2,038	1,981	2,092	19,885	19,208	20,542	9.76	9.42	10.12
Republic of Korea	1,692	1,615	1,764	19,833	18,762	20,762	11.72	11.08	12.41
Spain	2,291	2,274	2,308	24,533	24,289	24,764	10.71	10.59	10.82
Sweden	1,718	1,694	1,742	15,478	15,158	15,763	9.01	8.82	9.21
Switzerland	1,627	1,598	1,657	14,850	14,502	15,188	9.13	8.91	9.34
United States	1,819	1,814	1,823	24,272	24,190	24,346	13.35	13.30	13.39
Vietnam	1,351	941	1,744	25,513	15,696	35,570	18.88	11.94	29.52

Note: "Lower" means the lower bound of confidence interval (CI); "upper" means the upper bound of CI.
Abbreviations: 95% CI=95% confidence interval; YLL=years of life lost.

REFERENCES

1. Moran PAP. The estimation of standard errors in monte carlo simulation experiments. Biometrika 1975;62(1):1 – 4. http://dx.doi.org/10.1093/biomet/62.1.1.
2. Chiang CL. The life table and its applications. Malabar: Robert E. Krieger Publishing Company. 1984. https://openlibrary.org/books/OL3500112M/The_life_table_and_its_applications.
3. World Health Organization. WHO life tables by country. World Health Organization. 2018. https://www.who.int/data/gho/data/indicators/indicator-details/GHO/gho-ghe-life-tables-by-country. [2021-10-31].

4. United Nations. World population prospects 2019: highlights. 2019. https://www.un.org/development/desa/publications/world-population-prospects-2019-highlights.html. [2021-10-31].
5. World Health Organization. Coronavirus disease (COVID-2019) situation reports. 2022. https://www.who.int/emergencies/diseases/novel-coronavirus-2019/situation-reports. [2021-3-27].
6. CDC. Coronavirus disease 2019 (COVID-19). 2020. https://stacks.cdc.gov/view/cdc/89585. [2021-10-31].
7. National Health Commission of the People's Republic of China. The latest situation of the new coronavirus pneumonia epidemic situation as of 24:00 on June 30. 2020. http://www.nhc.gov.cn/xcs/yqtb/202007/a98e49570be24eaf88de98e6e6217fc8.shtml. [2021-10-31]. (In Chinese).
8. National Health Commission of the People's Republic of China. The latest situation of the new coronavirus pneumonia epidemic situation as of 24:00 on May 28. 2020. http://www.nhc.gov.cn/xcs/yqtb/202005/874765e641254eb4acea9d5e945f4e01.shtml. [2021-3-31]. (In Chinese).
9. The Norel Coronavirus Pneumonia Emergency Response Epidemiology Team. The epidemiological characteristics of an outbreak of 2019 novel coronavirus diseases (COVID-19) in China. Chin J Epidemiol 2020;41(2):145 – 51. http://dx.doi.org/10.3760/cma.j.issn.0254-6450.2020.02.003. (In Chinese).
10. Italy Higher Institute of Health. Integrated surveillance of COVID-19 in Italy. https://www.epicentro.iss.it/en/coronavirus/. [2021-10-31].
11. Republic of Korea MOHW. Coronavirus disease-19, Republic of Korea. 2020. http://ncov.mohw.go.kr/bdBoardList_Real.do?brdId=1&brdGubun=11&ncvContSeq=&contSeq=&board_id=&gubun=. [2021-3-31].
12. Ministry of Health, Social Services and Equality. Current situation. https://www.mscbs.gob.es/profesionales/saludPublica/ccayes/alertasActual/nCov-China/situacionActual.htm. [2021-10-31].
13. Robert Koch Institute. Coronavirus disease 2019 (COVID-19) daily situation report of the robert koch institute. 2022. https://www.rki.de/DE/Content/InfAZ/N/Neuartiges_Coronavirus/Situationsberichte/Gesamt.html. [2021-3-31].
14. CDC. Coronavirus disease 2019 (COVID-19). 2022. https://www.cdc.gov/coronavirus/2019-ncov/cases-updates/cases-in-us.html. [2021-3-31].
15. GitHub. Coronavirus-data. 2020. https://github.com/topics/coronavirus-data. [2021-3-31].
16. The Public Health Agency of Sweden. Confirmed cases in Sweden - daily update. 2022. https://www.folkhalsomyndigheten.se/smittskydd-beredskap/utbrott/aktuella-utbrott/covid-19/bekraftade-fall-i-sverige. [2021-3-31].
17. Norwegian Institute of Public Health. Daily report and statistics about coronavirus and COVID-19. 2020. https://www.fhi.no/en/id/infectious-diseases/coronavirus/daily-reports/daily-reports-COVID19/. [2021-3-31].
18. Australia ABC. Charting the COVID-19 spread in Australia. 2020. https://www.abc.net.au/news/2020-03-17/coronavirus-cases-data-reveals-how-covid-19-spreads-in-australia/12060704?nw=0. [2020-3-31].
19. Government of Canada. Epidemiological summary of COVID-19 cases in Canada. 2022. https://health-infobase.canada.ca/covid-19/epidemiological-summary-covid-19-cases.html. [2021-3-31].
20. Ministry of Health, Singapore. COVID-19 statistics. 2022. https://www.moh.gov.sg/covid-19/statistics. [2021-3-31].
21. Singapore COVID19. Dashboard of the COVID-19 virus outbreak in Singapore. 2022. https://co.vid19.sg/singapore/. [2020-3-31].
22. World Health Organization. WHO coronavirus disease (COVID-19) dashboard. 2022. https://covid19.who.int/. [2021-3-31].
23. COVID-19 information and resources. https://corona.go.jp/en/dashboard/.
24. Coronavirus dashboard, Netherlands. https://coronadashboard.government.nl/. [2021-3-31].
25. COVID-19 Switzerland. 2022. https://www.covid19.admin.ch/en/overview. [2021-3-31].
26. Belgium COVID-19 epidemiological situation. 2022. https://datastudio.google.com/embed/reporting/c14a5cfc-cab7-4812-848c-0369173148ab/page/ZwmOB. [2021-3-31].
27. Israel COVID-19 data tracker, ministry of health, Israel. 2020. https://www.gov.il/en/departments/guides/information-corona. [2021-3-31].
28. Ireland's COVID-19 data hub, government of Ireland. https://covid19ireland-geohive.hub.arcgis.com/. [2021-3-31].
29. COVID-19: current cases, ministry of health, government of New Zealand. 2022. https://www.health.govt.nz/covid-19-novel-coronavirus/covid-19-data-and-statistics/covid-19-current-cases. [2021-3-31].
30. Data on COVID-19 epidemic in slovenia, government of Slovenia. 2022. https://www.gov.si/en/topics/coronavirus-disease-covid-19/actual-data/. [2021-3-31].

Commentary

Measuring the Effect of COVID-19 Pandemic on Mortality: Review and Prospect — China, 2021

Jinlong Lin[1]; Guogui Huang[2]; Yue Wei[1]; Lijun Pei[1,#]

ABSTRACT

Current progress in measuring the effect of the pandemic on mortality is limited. Few studies have comprehensively and systematically elucidated the mechanism through which the pandemic affects mortality and what indicators are valid to capture such an effect. This paper presents a comprehensive analysis regarding the multifaceted effects of coronavirus disease 2019 (COVID-19) on mortality and its measurements [i.e., confirmed deaths per million people (CDPMP), case fatality rate (CFR), infection fatality risk (IFR), excess mortality P-score (EMPS), and life expectancy (LE)]. It was revealed that both data collection efforts and measurements on mortality due to COVID-19 were far from perfect and discussed the importance of accurate, prompt, and accessible data by any government over the course of fighting against the COVID-19 pandemic. It is believed that the biggest challenge in measuring the effect of the COVID-19 pandemic on mortality lies not in the construction of indicators at the academic level, but in the collection of data at the practical level. Thus, it is suggested to take measures to better monitor the development of the pandemic and mitigate the increasing burdens borne by the public health systems by improving the tracking system of mortality, standardizing the diagnosis of COVID-19's deaths, and disclosing mortality data.

THE EFFECTS OF THE COVID-19 PANDEMIC ON MORTALITY

Few studies have comprehensively and systematically elucidated the mechanism through which the pandemic affects mortality. Therefore, we try to present a comprehensive analysis regarding the effect of COVID-19 on mortality and its measurement. More specifically, the multifaceted effects of the pandemic on mortality, including the positive effects and the negative effects, as well as the direct effects and the indirect effects, as is shown in Table 1. On one hand, the reduced mobility led to a decline in road traffic deaths, fewer respiratory diseases, and infectious diseases such as influenza and human hand-foot-mouth diseases (*1*–*2*). It was estimated that there were 600,000 fewer deaths from non-COVID-19 causes globally in 2020 (*3*). On the other hand, the COVID-19 pandemic also had a negative effect on mortality. According to *World Health Statistics 2021*, COVID-19 has become the leading cause of death globally. It was estimated that the total number of global excess deaths directly and indirectly attributable to the COVID-19 pandemic in 2020 was at least 3 million, far more than the 1.8 million reported COVID-19 deaths that year (*4*).

The negative effects of the pandemic on mortality can be divided into direct and indirect effects. First is death due directly to COVID-19 because of acute respiratory distress syndrome and multiple organ dysfunction syndromes. Health conditions play a key role in influencing complications severity in COVID-19. Thus, its mortality is thought to be related to public health and demographic characteristics. Take Italy as an example, its higher population of older patients with COVID-19 infection illustrates why there is higher mortality (*5*). Clinical studies also reported that pre-existing cardiovascular disease seems to be linked with an increased risk of death in patients with COVID-19 (*6*).

Second, the pandemic also has an indirect negative effect on mortality. In many countries, disease screening has been suspended and routine diagnosis has been deferred as a result of the COVID-19 pandemic. Patients who are wary of being infected appear to be more reluctant to seek healthcare services (*7*), which has led to a substantial increase in the number of avoidable deaths. In the UK, for example, a number of avoidable cancer deaths are to be expected due to delays in diagnosis (*8*). Beyond the cancer cases, inappropriate anti-pandemic policy led to the provision of suboptimal care, which may have a larger effect on the wider population of patients with various

TABLE 1. The effect of the COVID-19 pandemic on mortality.

Effect type	Manifestation	Cause
Positive effect	Decline in road traffic deaths, fewer respiratory diseases, and some infectious diseases such as influenza	Reduced mobility due to traffic control, home isolation and NPIs
Negative effect		
Direct way	Rise in the number of deaths in patients with COVID-19	Mostly because of ARDS and MODS
Indirect way	Increases risk of death in patients with non-COVID-19 complications	Inappropriate policy which affects disease screening and diagnosis

Abbreviations: COVID-19=coronavirus disease 2019; NPIs=non-pharmaceutical interventions; ARDS=acute respiratory distress syndrome; MODS=multiple organ dysfunction syndrome.

diseases, like heart disease and stroke (*9*–*10*). Therefore, improper allocation of health care resources may also lead to a public health crisis because of non-COVID-19 health complications.

MAJOR INDICATORS IN MEASURING THE COVID-19 PANDEMIC EFFECT ON MORTALITY

Considering that the effect of the COVID-19 pandemic on mortality is very complicated, we used different indicators to reflect the various effects. The most common indicators are confirmed deaths per million people (CDPMP), case fatality rate (CFR), infection fatality risk (IFR), excess mortality P-score (EMPS), and life expectancy (LE). We tried to review and compare these four widely used mortality indicators regarding their efficacy in gauging the effect of COVID-19 on mortality and the appropriate contexts for using these indicators.

CDPMR is the simplest indicator. The number of confirmed COVID-19 deaths reflects the direct loss of life caused by the disease. It is often needed to adjust for the size of the population by dividing by one million, especially when comparing across countries. CFR and IFR are the most widely discussed indicators during the pandemic. Of the two, CFR is the proportion of confirmed COVID-19 deaths within a defined follow-up population (i.e., actual infections), mainly reflecting the severity of COVID-19 that causes death. However, CFR only focuses on confirmed cases, which may omit statistics on minor infections. Therefore, it may be better for us to use IFR, the ratio of death cases to all cases (including undetected instances), to reflect the risk of dying from COVID-19.

Although these three indicators quantify the overall scale of COVID-19 to a certain extent, they are limited as comprehensive measures, since they can only reflect the negative effect of the COVID-19 pandemic on mortality in a direct way. From this perspective, EMPS and LE are the more comprehensive measures reflecting the total effect of the pandemic on mortality.

EMPS is calculated based on excess deaths, the number of all-cause deaths during the pandemic period beyond the expected deaths under non-COVID-19 conditions, measured as the difference between reported deaths and expected deaths. Hence, it is only needed to count all the deaths within the year, without distinguishing the cause of deaths, whereas it is hard to ensure the accuracy of the numerator and the denominator in estimating CFR and IFR. For better comparisons across countries when there are large differences in population, it is required to divide the excess deaths by the expected deaths to get P-Score. Hence, the formula of EMPS is written as "EMPS = (reported deaths – expected deaths) / expected deaths × 100". However, demographic differences also add to the complexity in drawing comparisons when using EMPS. In this case, it is helpful to use the LE indicator to investigate the total effect of the COVID-19 pandemic on mortality. Unlike other indicators, LE is not affected by demographic characteristics, as it is calculated based on age-specific mortality rates by sex, so it could be used for direct comparison between different populations.

These indicators have been applied to measure the COVID-19 pandemic effect on mortality to varying degrees worldwide since the outbreak of the COVID-19, but the progress is still very limited. We believe that the fundamental problem lies in the operation of population statistics.

INSUFFICIENT TESTING VOLUMES IN LOW- AND LOWER MIDDLE-INCOME COUNTRIES

Although testing capacity has increased substantially worldwide, access to COVID-19 testing in most low- and lower middle-income countries is still in shortage due to high costs. Take Kenya as an example, the average cost for a patient seeking a test achieved $11,

the equivalent of 6 days' wages for a Kenyan living in extreme poverty (*11*). A special survey conducted by the COVID-19 Clinical Research Coalition showed that low access outside major cities and shortage of test kits also added obstacles to COVID-19 testing in such countries. Nearly 90% of the subjects believed that diagnostics needed to be used more widely and made more available (*12*). The limited testing would lead to huge differences between reported confirmed deaths and actual deaths, which has leaved an adverse effect on the assessment and response to the pandemic.

REFLECTING ACTUAL RISK OF DYING FROM COVID-19

With the rapid progress of vaccine coverage, it is particularly important to do the assessment of mortality risk and the evaluation of pandemic prevention and control effects, which may guide the allocation of vaccines around the world. However, it is difficult to measure and compare the true mortality risk of COVID-19 across countries. One reason is that the mortality risk varied with time and populations vastly. For example, CFR and IFR reported by many countries have varied substantially over time. According to Johns Hopkins CSSE, the CFR of Germany population has ranged from 0.17% to 4.70%, while that of Italy has ranged from 1.94% to 14.52% from February 21, 2020 to November 6, 2021. Meanwhile, findings from seroprevalence data showed that IFR ranged from 0 to 1.63% among 74 estimates and the medium rate was 0.27% (*13*). Another example might be the evidence that minority ethnic groups are at a higher risk of catching and dying from COVID-19. Data from the United Kingdom Office for National Statistics showed that the risk of dying from COVID-19 for black people was more than 4 times the white population in England and Wales (*14*). The changes in CFR and IFR are thought to be associated with many factors like demographic, economic, and political variables (*15*–*16*). The variability of CFR and IFR added to the difficulty in the evaluation and management of the pandemic.

LIMITED PROGRESS IN THE COLLECTION AND PUBLISHING OF ALL-CAUSE DEATH DATA

The analysis of the overall effect of the COVID-19 pandemic on mortality was based on the collection and publication of all-cause death data. Take the indicator LE as an example, only some countries have published the data of LE in 2020 so far, although such work is beneficial for managing the pandemic. According to Eurostat, LE at birth fell in the vast majority of European Union due to the COVID-19 pandemic. The largest decreases were recorded in Spain (-1.6 years compared with 2019), followed by Bulgaria (-1.5). The indicator LE clearly reflected the offsetting effect of the pandemic on the positive progress of public health in EU countries (*17*). However, we still lacked official statistics on LE for more countries to understand the global situation. Up to now, there have been two main databases publishing all-cause death data regularly, the Human Mortality Database (HMD) and the World Mortality Dataset (WMD). WMD has been publishing updates since January 2021 for 108 countries and regions currently. However, the data is not broken down by age and published either weekly or monthly. HMD has been publishing relatively detailed updates since May 2020, but it has only involved 41 countries or areas so far. Lack of timely, detailed data sources will no doubt hinder the application of EMPS and LE as well as understanding the ongoing pandemic, eventually turning into a major problem for researchers and policymakers.

DISCUSSCION AND FUTURE DIRECTIONS

We need more timely, accurate, and accessible COVID-19 mortality data from surveillance systems to aid in the evaluation and management of the pandemic. Especially as variants such as Omicron become dominant, many countries across the world have experienced a surge in deaths since 2021. Although EMPS and LE were less susceptible to limitations in these systems based on COVID-19 diagnosis, they did not realize the expected value in understanding the burden of COVID-19, because of limited collection of all-cause death data in most developing countries. Therefore, further investment to improve the timely recording and cause diagnosis of deaths is a vital part of pandemic preparedness for most countries.

First, equitable access to vaccines and diagnostics in low- and lower middle-income countries must be ensured. Research showed a sustained reduction in COVID-19 mortality corresponding to increasing vaccines coverage and testing volumes (*18*–*19*).

However, the production and purchasing capacity of vaccines and diagnostics varies vastly in high- and low-income countries, leaving a negative effect on the evaluation and management of the pandemic across countries.

Second, proper death certification and registration should be encouraged for every country. The accuracy of the confirmed COVID-19 death data remains to be discussed, due to the limited testing and challenges in the attribution of the cause of deaths. Improper death certification and registration will reduce the data quality and limit the ability to track the evolving COVID-19 pandemic, which in turn adversely affect the local and national responses. So far, most countries still have been typically providing own guidance on how and when to report confirmed COVID-19 deaths, and some countries are still slow in constructing death registration systems. In order to obtain more accurate and comparable death data, countries are suggested to establish uniform standards for COVID-19 death certification while improving death registration.

Third, all-cause death data should be effectively collected and disclosed. The calculation and comparison of all-cause mortality across countries was not affected by limitations such as insufficient testing volumes. Therefore, using all-cause death data to analyze the effect of the epidemic on mortality is currently the most likely to be achieved on a global scale. Currently, the database HMD and WMD are collecting all-cause death data from various countries or regions, but this depends on the timely and transparent data released by each government.

In summary, measuring the mortality variations during the COVID-19 pandemic can contribute to control of the pandemic. This requires us to fully understand the mechanism of the effect of the COVID-19 pandemic on mortality and choose proper measurement to capture this impact. Most importantly, effective measures must be taken to effectively and promptly collect data on various measurements.

Conflicts of Interest: No conflicts of interest.

Funding: Supported by grants from the National Natural Science Foundation of China (41871360), and National Key Research and Development Program of China (2018YFC1004303).

doi: 10.46234/ccdcw2022.110

[#] Corresponding author: Lijun Pei, peilj@pku.edu.cn.

[1] Institute of Population Research, China Center on Population Health and Development, Peking University, Beijing, China; [2] Macquarie Business School, Macquarie University, Sydney, Australia.

Submitted: November 29, 2021; Accepted: June 03, 2022

REFERENCES

1. Calderon-Anyosa RJC, Kaufman JS. Impact of COVID-19 lockdown policy on homicide, suicide, and motor vehicle deaths in Peru. Prev Med 2021;143:106331. http://dx.doi.org/10.1016/j.ypmed.2020.106331.
2. Huh K, Kim YE, Ji W, Kim DW, Lee EJ, Kim JH, et al. Decrease in hospital admissions for respiratory diseases during the COVID-19 pandemic: a nationwide claims study. Thorax 2021;76(9):939 – 41. http://dx.doi.org/10.1136/thoraxjnl-2020-216526.
3. World Health Organization. World health statistics 2021: monitoring health for the SDGs, sustainable development goals. Geneva: World Health Organization; 2021. Licence: CC BY-NC-SA 3.0 IGO. https://apps.who.int/iris/bitstream/handle/10665/342703/9789240027053-eng.pdf.
4. Troeger C. Just how do deaths due to COVID-19 stack up? 2021. https://www.thinkglobalhealth.org/article/just-how-do-deaths-due-covid-19-stack. [2021-9-30].
5. Onder G, Rezza G, Brusaferro S. Case-fatality rate and characteristics of patients dying in relation to COVID-19 in Italy. JAMA 2020;323(18):1775 – 6. http://dx.doi.org/10.1001/jama.2020.4683.
6. Nishiga M, Wang DW, Han YL, Lewis DB, Wu JC. COVID-19 and cardiovascular disease: from basic mechanisms to clinical perspectives. Nat Rev Cardiol 2020;17(9):543 – 58. http://dx.doi.org/10.1038/s41569-020-0413-9.
7. Richards M, Anderson M, Carter P, Ebert BL, Mossialos E. The impact of the COVID-19 pandemic on cancer care. Nat Cancer 2020;1(6):565 – 67. http://dx.doi.org/10.1038/s43018-020-0074-y.
8. Maringe C, Spicer J, Morris M, Purushotham A, Nolte E, Sullivan R, et al. The impact of the COVID-19 pandemic on cancer deaths due to delays in diagnosis in England, UK: a national, population-based, modelling study. Lancet Oncol 2020;21(8):1023 – 34. http://dx.doi.org/10.1016/S1470-2045(20)30388-0.
9. Ganatra S, Dani SS, Shah S, Asnani A, Neilan TG, Lenihan D, et al. Management of cardiovascular disease during coronavirus disease (COVID-19) pandemic. Trends Cardiovasc Med 2020;30(6):315 – 25. http://dx.doi.org/10.1016/j.tcm.2020.05.004.
10. Bersano A, Kraemer M, Touzé E, Weber R, Alamowitch S, Sibon I, et al. Stroke care during the COVID-19 pandemic: experience from three large European countries. Eur J Neurol 2020;27(9):1794 – 800. http://dx.doi.org/10.1111/ene.14375.
11. Connor A, Hariharan N, Carson S, Sanders KC, Vosburg KB, Sabot O. Access to COVID-19 testing in low- and middle-income countries is still critical to achieving health equity. Health Affairs Blog. 2021. https://www.healthaffairs.org/do/10.1377/forefront.20211026.483412. [2021-11-7].
12. COVID-19 Clinical Research Coalition. A snapshot of COVID-19 diagnostics access and availability in low- and middle-income countries. 2021. https://covid19crc.org/wp-content/uploads/2021/08/Coalition-Diagnostics-Survey-results-report-_-FINAL.pdf. [2021-11-7].
13. Ioannidis JPA. Infection fatality rate of COVID-19 inferred from seroprevalence data. Bull World Health Organ 2021;99(1):19 – 33F. http://dx.doi.org/10.2471/BLT.20.265892.
14. Office for National Statistics. Coronavirus (COVID-19) related deaths by ethnic group, England and Wales: 2 March 2020 to 15 May 2020. 2020. https://www.ons.gov.uk/peoplepopulationandcommunity/birthsdeathsandmarriages/deaths. [2021-11-9].
15. COVID-19 Forecasting Team. Variation in the COVID-19 infection–fatality ratio by age, time, and geography during the pre-vaccine era: a systematic analysis. Lancet 2022;399(10334):1469 – 88. http://dx.doi.org/10.1016/S0140-6736(21)02867-1.
16. Cao Y, Hiyoshi A. Montgomery S COVID-19 case-fatality rate and demographic and socioeconomic influencers: worldwide spatial

regression analysis based on country-level data. BMJ Open 2020;10(11):e043560. http://dx.doi.org/10.1136/bmjopen-2020-043560.
17. Eurostat. File: table1 Life expectancy at birth.png. 2022. https://ec.europa.eu/eurostat/statistics-explained/index.php?title=File:Table1_Life_expectancy_at_birth.png. [2021-6-3].
18. Bernal JL, Andrews N, Gower C, Robertson C, Stowe J, Tessier E, et al. Effectiveness of the Pfizer-BioNTech and Oxford-AstraZeneca vaccines on covid-19 related symptoms, hospital admissions, and mortality in older adults in England: test negative case-control study. BMJ 2021;373:n1088. http://dx.doi.org/10.1136/bmj.n1088.
19. Wei C, Lee CC, Hsu TC, Hsu WT, Chan CC, Chen SC, et al. Correlation of population mortality of COVID-19 and testing coverage: a comparison among 36 OECD countries. Epidemiol Infect 2021;149:e1. http://dx.doi.org/10.1017/S0950268820003076.

Methods and Applications

Field Evaluation of a Duplex RT-RAA Assay for Rapid Detection of SARS-CoV-2 — Hebei Province, China, January 2021

Ruiqing Zhang[1,&]; Shunxiang Qi[2,&]; Jiandong Li[1]; Shiyou Liu[2]; Guangyue Han[2]; Xinxin Shen[1]; Qi Li[2,#]; Wenbo Xu[1,#]; Xuejun Ma[1,3,#]

ABSTRACT

Introduction: Recently, a local cluster epidemic has occurred in Shijiazhuang City, Hebei Province. Failure to promptly identify patients with fever in rural areas was the major reason for this epidemic.

Methods: We presented the field evaluation of a new real-time reverse transcription recombinase-aided amplification (RT-RAA) kit incorporating an endogenous internal control in a single-tube format, completed at the Hebei CDC from January 17, 2021 to January 27, 2021.

Results: We evaluated the diagnostic performance of RT-RAA assay using automatic extracted RNA of 808 clinical samples. Compared with reverse transcriptase real-time quantitative PCR (qRT-PCR), RT-RAA kit achieved 92.41% sensitivity, 98.78% specificity and a 96.29% coincidence rate, demonstrating an excellent agreement between the RT-RAA assay and qRT-PCR assay. Furthermore, 58 samples were extracted using a manual extraction method within 5 minutes, but only samples with high nucleic acid concentration (cycle threshold value not higher than 32) could be stably detected.

Discussion: The RT-RAA is more suitable to meet the needs of rapid, sensitive, and accurate detection in community-level medical institutions.

INTRODUCTION

Recently, local cluster COVID-19 epidemics have occurred in rural areas and the urban-rural border regions in Shijiazhuang City, Hebei Province. Rural medical institutions were not able to detect new cases promptly, resulting in rapid spread of the epidemic (*1*).

Reverse transcriptase real-time quantitative PCR (qRT-PCR) is considered the gold standard of severe acute respiratory syndrome coronavirus 2 (SARS-CoV-2) RNA detection. However, it is difficult to be used at the grass roots level due to being relatively time-consuming and requiring skillful technicians, specialized equipment, and biosafety labs (*2*–*3*). In our previous study, we reported an ultrafast single-tube assay for SARS-CoV-2 RNA detection using a reverse transcription recombinase-aided amplification (RT-RAA) kit, which revealed the distinctive advantages of simplicity and rapidity in terms of operation and turnaround time (*4*). We then upgraded this kit and developed a duplex single-tube assay for SARS-CoV-2 RNA targeting both the ORF1ab gene and GAPDH gene (endogenous internal control). The RT-RAA kit passed the quality assessment of National Institutes for Food and Drug Control and showed the lowest detection sensitivity in the range of 45 copies/mL to 137 copies/mL on November 30, 2020. Afterwards, the kit obtained the CE certification of the European Union and was officially approved by National Medical Products Administration (NMPA). Here we presented the onsite evaluation results of the RT-RAA kit, completed in Hebei CDC from January 17, 2021 to January 27, 2021.

MATERIALS AND METHODS

Specimens

The specificity evaluation panel was preserved in China CDC consisting of inactivated cultures or nucleic acids of SARS-CoV-2, human coronavirus (HKU1, OC43, NL63, and 229E), influenza virus types A (Flu A), FluA-H1N1, FluA-H3N2, FluA-H5N1, FluA-H7N9, influenza virus types B, respiratory syncytial virus type A and B, parainfluenza virus, human rhinovirus type A, type B, and type C, human adenovirus, enteroviruses, human metapneumovirus, Epstein-Barr virus, measles virus, human cytomegalo virus, Boca virus, rotavirus, norovirus, mumps virus, varicella zoster virus, *Mycoplasma pneumoniae*, *Chlamydia pneumoniae*, *Legionella pneumophilia*, *Bordetella pertussis*, *Haemophilus influenzae*, *Staphylococcus aureus*,

Streptococcus pneumoniae, *Streptococcus pyogenes*, *Klebsiella pneumoniae*, *Mycobacterium tuberculosis*, *Aspergillus fumigatus*, *Candida albicans*, *Candida glabrata*, *Cryptococcus neoformans* and human genome DNA.

A total of 808 throat swab samples were collected in Hebei from January 17, 2021, to January 27, 2021. National Reference Panel for 2019-nCoV Nucleic Acids Detection Kit was from NMPA. All aspects of the study were performed as per the National Code of Ethics and approved by the Institutional Review Boards of local CDCs and hospital mentioned above.

Analytical Sensitivity and Specificity of RT-RAA Kit

The schematic diagram of the endogenous internal controlled RT-RAA was shown in Figure 1. All of the primers and probes for the ORF1ab gene and GAPDH gene (*5*) were lyophilized in the reaction unit. The specificity evaluation panel as described above was used to evaluate the specificity of RT-RAA assay. The original concentration of National Reference S solution was 3×10^5 copies/mL. The sensitivity of RT-RAA assay was assessed using 3-fold serially diluted S solution (1∶9, 1∶27, 1∶81, 1∶243, 1∶729, and 1∶2,187, labeled as S1–S6, respectively). Nucleic acid extraction of each S concentration was then carried out for eight replicates by RT-RAA detection.

Automatic RNA Extraction

Total RNA was extracted from 200 μL of sample preservation solution using automatic extraction kits (BioPerfectus, China) according to the instructions recommended by the manufacturer. The nucleic acid was eluted in 50 μL of nuclease-free water and stored at -80 °C until use.

Simplified RNA Extraction

RNA was obtained from 58 clinical samples using nucleic acid lysis solution (Qi Tian, Jiangsu Province, China) under the following dilution: 95 μL of clinical samples mixed with 5 μL of lysis solution. The mixtures were then briefly vortexed and incubated at room temperature for 2 min, followed by centrifugation (10,000 rpm) prior to use. Among them, 10 samples were collected in sampling tubes from Changchun Zhihe Co., Ltd, China and the other 48 samples were collected in sampling tubes from Cangzhou Yongkang Co., Ltd., China.

Protocol of RT-RAA Kit for SARS-CoV-2 RNA Detection

A RT-RAA reaction system included 42.5 μL of reaction buffer, 2.5 μL of 280 mmol/L magnesium acetate, 5 μL of extracted nucleic acid or 5 μL negative/positive control. After capping the tube, the reaction tube was symmetrically placed in the pretreatment system RAA-B6108 for pre-defined vortex and centrifugation for 7 min, the reaction tube was then removed and transferred to the nucleic acid amplification detector RAA-F1620. The reaction temperature was set at 39 ℃ for 15 min, and the results could be observed in real time.

The result was considered positive when ORF1ab channel was positive and GAPDH was positive or negative. The result was considered negative when

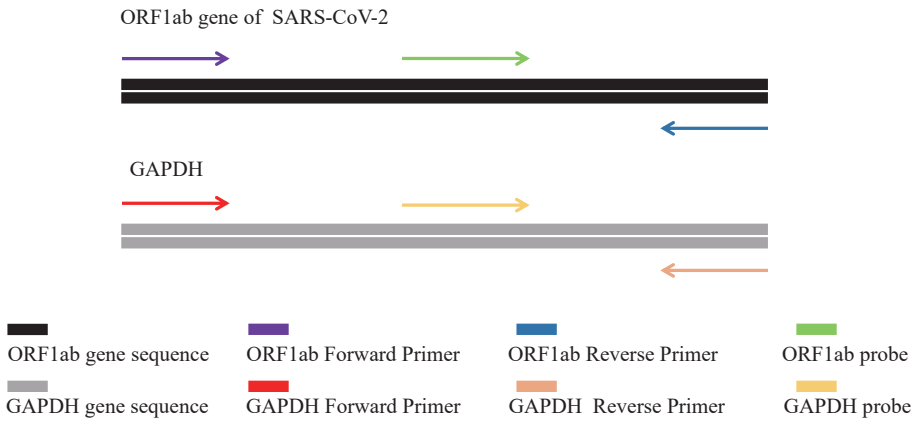

FIGURE 1. Schematic diagram of the endogenous internal controlled RT-RAA assay for detection of SARS-CoV-2.
Abbreviations: RT-RAA=reverse transcription recombinase-aided amplification; SARS-CoV-2=severe acute respiratory syndrome coronavirus 2; GAPDH=glyceraldehyde-3-phosphate dehydrogenase.

ORF1ab channel was negative and GAPDH was positive. The sample needed to be re-tested when both target genes (ORF1ab and GAPDH) were negative, probably resulting from the presence of inhibitors in the sample or the sampling errors.

Operation Standard

All the experimental operations and biosafety protection in this study strictly abided by Novel Coronavirus Nucleic Acid Testing Work Manual for Medical Institutions (2nd Edition) (*6*) and SARS-CoV-2 Laboratory Biosafety Guidelines (2nd Edition) (*7*) issued by National Health Commission of the People's Republic of China.

Statistical Data Analysis

COVID-19 prevention and control protocols (8th Edition) recommended that confirmed cases of COVID-19 infection should be identified by qRT-PCR kits (*6*). The qRT-PCR kit (BioGerm, Shanghai) approved by NMPA was selected in this study for parallel experiment. SPSS Statistics software (version 21, IBM, NY, USA) was used to perform the statistical analysis. The results of qRT-PCR assay and RT-RAA assay were analyzed using Kappa and McNemar's tests, and a value of $P<0.05$ was considered statistically significant. Scatter diagram analysis was used to analyze the relationship between the time threshold (min) detected by RT-RAA and the cycle threshold (Ct) of qRT-PCR method using 292 positive samples of both assays.

RESULTS

Sensitivity and Specificity of the RT-RAA Kit

S1–S6 produced positive results for all 8 replicates, and the sensitivity of RT-RAA was 137 copies/mL (S6) as shown in Figure 2. No cross reactions with four common coronaviruses or other viral and bacterial pathogens were observed.

Comparison of RT-RAA and qRT-PCR

Totally, 808 samples were extracted using automatic RNA extraction kits and detected by RT-RAA and qRT-PCR (Table 1). Among the 808 samples, RT-RAA results for 778 samples were consistent with qRT-PCR (292 were positive, 486 were negative) and

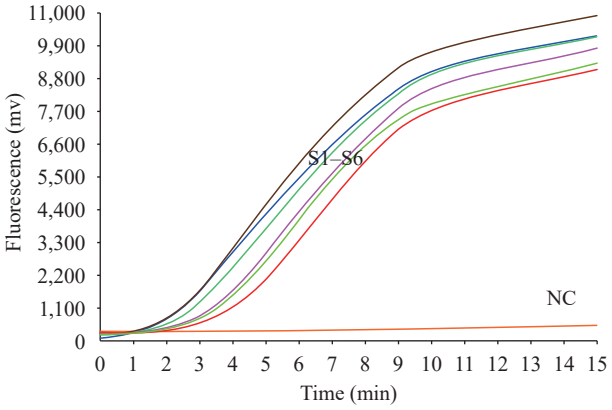

FIGURE 2. Sensitivity of the duplex RT-RAA assays for SARS-CoV-2 RNA using diluted National Reference (S1–S6).
Note: The blue curve represents National Reference S1 (33,333 copies/mL); the brown curve represents National Reference S2 (11,111 copies/mL); the dark green curve represents National Reference S3 (3,703 copies/mL); the purple curve represents national reference S4 (1,234 copies/mL); the light green curve represents national reference S5 (411 copies/mL); the red curve represents national reference S6 (137 copies/mL).
Abbreviations: SARS-CoV-2=severe acute respiratory syndrome coronavirus 2; RT-RAA=reverse transcription recombinase-aided amplification.

TABLE 1. The clinical performance of the RT-RAA using simplified RNA extraction or automatic RNA extraction compared with qRT-PCR as the reference method.

Method		qRT-PCR		Performance characteristics		
		Positive	Negative	Sensitivity (%)	Specificity (%)	Kappa
RT-RAA (automatic RNA extraction)	Positive	292	6	92.41	98.78	0.92
	Negative	24	486			
	Total (n=808)	316	492			
RT-RAA (simplified RNA extraction)	Positive	12	0	40	100	0.39
	Negative	18	28			
	Total (n=58)	30	28			

Abbreviations: RT-RAA=reverse transcription recombinase-aided amplification; qRT-RAA=reverse transcriptase real-time quantitative PCR.

30 were inconsistent (6 were RT-RAA positive only and 24 were qRT-PCR positive only). These 24 samples were positive only by qRT-PCR but negative by RT-RAA, and the corresponding Ct values were all distributed between 35 and 40. Compared with qRT-PCR, the sensitivity of RT-RAA was 92.41% and the specificity was 98.78%. The total coincidence rate was 96.29% and the Kappa was 0.92 (P<0.05). As shown in Figure 3, we observed that the fluorescence signal of most samples reached the threshold within 4 min. Most of the samples with low viral load (Ct≥35) had higher threshold time values within 10 min, plus the pre-reaction of 7 min, the duration of total process was within 20 min.

Furthermore, 58 samples were extracted using simplified extraction method and detected by RT-RAA and qRT-PCR (Table 1). Among the 58 samples, RT-RAA results of 40 samples were consistent with qRT-PCR (12 were positive, 28 were negative), and the Ct values of 12 RT-RAA-positive samples ranged from 20 to 32. Additionally, the Ct values of 18 samples (positive only by qRT-PCR) ranged from 32.2 to 36.4.

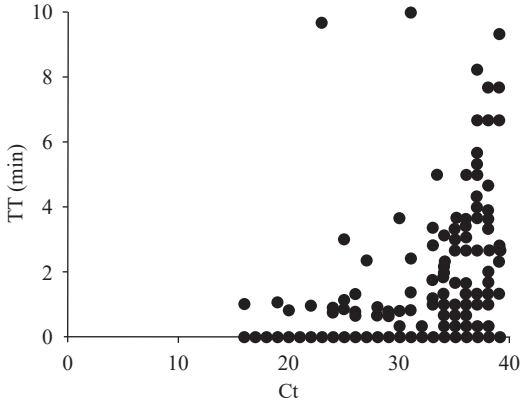

FIGURE 3. Scatter diagram analysis of RT-RAA threshold time (TT) (y-axis) and qRT-PCR cycle threshold values (Ct) (x-axis).
Note: Data were analyzed by GraphPad Prism software (version 8, GraphPad Software, San Diego, USA).
Abbreviations: RT-RAA=reverse transcription recombinase-aided amplification; qRT-PCR=reverse transcriptase real-time quantitative PCR.

DISCUSSION

At present, commercial qRT-PCR kits are widely used for the detection of SARS-CoV-2 (*8*–*9*). Our current results indicated that the clinical performance of the RT-RAA kit was comparable to that of the qRT-PCR kit. Nevertheless, the samples with Ct≥35 were steadily detected by RT-RAA within 20 min, much shorter than qRT-PCR kits (1–2 h), suggesting that RT-RAA assay had adequate sensitivity to rapidly identify clinical samples with very low viral load (*4*). This RT-RAA kit incorporated an endogenous internal control that ensured its reliability by monitoring sample collection, RNA extraction, and RAA reaction. With added advantages of simple operation, quick training, and portability, RT-RAA is thus a valuable alternative to qRT-PCR to meet the needs of rapid, sensitive, and accurate detection in community-level medical institutions (such as fever clinic, county, and township) (*10*–*11*).

We observed that the selection of nucleic acid extraction methods had a dramatic impact on the sensitivity of RT-RAA detection. Particularly, the extraction efficiency and quality of sampled nucleic acids are greatly affected by the virus sampling tubes with inactivation agents. The influence of sampling tubes could be eliminated by using a fully automatic nucleic acid extraction instrument and a matching extraction kit. While using a simplified extraction method, the sensitivity of RT-RAA dropped to 40%, suggesting that the RT-RAA was not compatible with the inactivator of sampling tubes. At present, RT-RAA is only moderately suitable for simplified extracted nucleic acid with a few brands of sampling tubes containing inactivated agents (such as Changchun Zhihe Biotechnology Co., LTD.). The use of nucleic acid lysis solution could achieve manual extraction of nucleic acid within 5 mins, but only samples with a high nucleic acid concentration (Ct value not higher than 32) could be stably detected.

However, this study had a few limitations. Firstly, only single gene (ORF1ab) was targeted for SARS-CoV-2. Secondly, this study only tested 58 throat swab samples using simplified RNA extraction, different clinical sample types and more samples are needed to verify this method.

Our clinical evaluation results highlighted the feasibility of RT-RAA and its potential utilization in rural areas. Herein, we propose two schemes for practical reference. Scheme 1: this combination (Any sampling tube with inactivation agent + fully automated nucleic acid extraction instrument + RT-RAA kit) is recommended for routine use in county health centers and fever clinic laboratories equipped with biosafety cabinets. Scheme 2: this combination (Sampling tube from Changchun Zhihe Biotechnology Co., LTD. + 5 min of manual simplified extraction + RT-RAA kit) is recommended for emergency use in township health centers and fever outpatient

laboratories without biosafety cabinets.

Conflicts of Interest: No conflicts of interest declared.

Acknowledgements: Hebei Center for Disease Control and Prevention.

Funding: Supported by grants from National institute for viral disease control and prevention, China CDC (2019HYDQNJJ03) and the key R&D projects in Zibo City (2020kj100011).

doi: 10.46234/ccdcw2022.111

[#] Corresponding authors: Qi Li, liqinew@126.com; Wenbo Xu, wenbo_xu1@aliyun.com; Xuejun Ma, maxj@ivdc.chinacdc.cn.

[1] National Institute for Viral Disease Control and Prevention, China CDC, Beijing, China; [2] Hebei Center for Disease Control and Prevention, Shijiazhuang City, Hebei Province, China; [3] Center for Biosafety Mega-Science, Chinese Academy of Sciences, Wuhan City, Hubei Province, China.
[&] Joint first authors.

Submitted: October 18, 2021; Accepted: May 20, 2022

REFERENCES

1. Wang BN, Zheng H. From blanket quarantine in Wuhan to distant centralized quarantine in Shijiazhuang: the evolution of China's COVID-19 quarantine approach. Infection 2021;49(4):765 – 7. http://dx.doi.org/10.1007/s15010-021-01623-8.
2. Wu T, Ge YY, Zhao KC, Zhu XJ, Chen Y, Wu B, et al. A reverse-transcription recombinase-aided amplification assay for the rapid detection of N gene of severe acute respiratory syndrome coronavirus 2(SARS-CoV-2). Virology 2020;549:1 – 4. http://dx.doi.org/10.1016/j.virol.2020.07.006.
3. Xue GH, Li SL, Zhang WW, Du B, Cui JH, Yan C, et al. Reverse-transcription recombinase-aided amplification assay for rapid detection of the 2019 novel coronavirus (SARS-CoV-2). Anal Chem 2020;92 (14):9699 – 705. http://dx.doi.org/10.1021/acs.analchem.0c01032.
4. Wang J, Cai K, He X, Shen X, Wang J, Liu J, et al. Multiple-centre clinical evaluation of an ultrafast single-tube assay for SARS-CoV-2 RNA. Clin Microbiol Infect 2020;26(8):1076 – 81. http://dx.doi.org/10.1016/j.cmi.2020.05.007.
5. Adeola F. Normalization of gene expression by quantitative RT-PCR in human cell line: comparison of 12 endogenous reference genes. Ethiop J Health Sci 2018;28(6):741 – 8. http://dx.doi.org/10.4314/ejhs.v28i6.9.
6. Liu FF , Zheng CJ, Wang LP, Geng MJ, Chen H, Zhou S, et al. Interpretation of the Protocol for Prevention and Control of COVID-19 in China (Edition 8). China CDC Weekly 2021;3(25):527 – 30. http://dx.doi.org/10.46234/ccdcw2021.138.
7. National Health Commission of the People's Republic of China. SARS-CoV-2 laboratory biosafety guidelines 2020. http://www.nhc.gov.cn/yzygj/s7659/202012/b89bcd0813da41788688eb14787b3c72.shtml. [2022-5-19].
8. Krüttgen A, Cornelissen CG, Dreher M, Hornef MW, Imöhl M, Kleines M. Comparison of the SARS-CoV-2 Rapid antigen test to the real star Sars-CoV-2 RT PCR kit. J Virol Methods 2021;288:114024. http://dx.doi.org/10.1016/j.jviromet.2020.114024.
9. Okamaoto K, Shirato K, Nao N, Saito S, Kageyama T, Hasegawa H, et al. Assessment of real-time RT-PCR kits for SARS-CoV-2 detection. Jpn J Infect Dis 2020;73(5):366 – 8. http://dx.doi.org/10.7883/yoken.JJID.2020.108.
10. Wang RH, Zhang H, Zhang Y, Li XN, Shen XX, Qi JJ, et al. Development and evaluation of recombinase-aided amplification assays incorporating competitive internal controls for detection of human adenovirus serotypes 3 and 7. Virol J 2019;16(1):86. http://dx.doi.org/10.1186/s12985-019-1178-9.
11. Bai XD, Ma XJ, Li MH, Li XN, Fan GH, Zhang RQ, et al. Field applicable detection of hepatitis B virus using internal controlled duplex recombinase-aided amplification assay and lateral flow dipstick assay. J Med Virol 2020;92(12):3344 – 53. http://dx.doi.org/10.1002/jmv.25778.

Methods and Applications

Novaferon Effectively Inhibits Ancestral SARS-CoV-2 and Omicron Variant *in Vitro*, 2022

Fei Ye[1]; Baoying Huang[1]; Li Zhao[1]; Yao Deng[1]; Jiao Ren[1]; Wenjie Tan[1,#]

ABSTRACT

Introduction: To identify Novaferon (Nova), a novel recombinant protein of interferon (IFN)-α, antiviral activity against ancestral severe acute respiratory syndrome coronavirus 2 (SARS-CoV-2) and Omicron variant *in vitro*.

Methods: Vero cells were infected with SARS-CoV-2 and Omicron variant in a biosafety level-3 laboratory. And viral replications were accessed using quantitative real-time reverse transcription polymerase chain reaction (RT-PCR).

Results: Results demonstrated that Nova has effective inhibition against ancestral SARS-CoV-2 and Omicron variant *in vitro*.

Discussion: The *in vivo* effects of Nova need to be further tested in animal models. And large-scale randomized double-blind clinical trials are needed to reveal its potentially clinical application.

INTRODUCTION

Coronavirus disease 2019 (COVID-19), caused by severe acute respiratory syndrome coronavirus 2 (SARS-CoV-2), has become a severe threat to global public health (*1*). The virus has spread rapidly to more than 200 countries worldwide. The World Health Organization (WHO) declared the outbreak of COVID-19 to be a global pandemic on March 11, 2020. As of February 15, 2022, the disease had caused more than 400,000,000 human infections with over 5,000,000 deaths globally (*2*). Moreover, the constant emergence of variants of concern (VOCs) of SARS-CoV-2, such as the Omicron (B.1.1.529) variant, increases the risk of vaccine failure (*3*). Thus, there is an urgent need for the development of antiviral drugs.

Type I interferons (IFNs) α / β are one of the most common biotechnological drugs that have broad-spectrum antiviral activities against ribonucleic acid (RNA) viruses. Type I IFNs induce an antiviral response across a wide range of cell types and mediate adaptive immune responses (*4*). SARS-CoV-2 replication is inhibited by IFN-α and IFN-β *in vitro* (*5*). Novaferon (Nova) is a new recombinant IFN-α-like protein with significantly higher activity than IFN-α; it has been approved for the treatment of chronic hepatitis B in China (*6*). In our previous study, Nova was shown to inhibit ancestral SARS-CoV-2 replication *in vitro* (*7*). The Nova and Nova plus lopinavir/ritonavir groups had significantly higher viral clearance rates than the lopinavir/ritonavir group and a 3-day reduction in viral clearance (*7*). The cytotoxic effect of Nova was assayed in this study, and we reported that Nova exhibited antiviral activity not only against ancestral SARS-CoV-2, but also against the Omicron variant in cultured cells. These results showed the therapeutic potency of type I IFNs against COVID-19.

METHODS

African green monkey kidney Vero cells (ATCC, CCL-81) were cultured at 37 °C in Dulbecco's modified Eagle's medium (DMEM) (Gibco, Grand Island, NY, USA) supplemented with 10% fetal bovine serum(FBS)(Gibco, Grand Island, NY, USA), 200 mg/mL streptomycin, and 200 IU/mL penicillin in an atmosphere containing 5% CO_2. SARS-CoV-2 viruses (ancestral virus 2019nCoV-CDC-Tan-HB01 and the Omicron variant 2019nCoV-CDC-Tan-GD01) were kept in our laboratory. The viruses were propagated in Vero cells. Viral titers were determined using a standard $TCID_{50}$ assay. All infection experiments were performed in a biosafety level-3 laboratory.

The cytotoxicity of Nova was determined in Vero cells using CCK8 assays (DOJINDO, Kumamoto, Japan). Briefly, Vero cells were seeded in 96-well plates and cultured overnight. Different concentrations of the compound solution (100 μL) in DMEM were added to the Vero cells and incubated for 48 h at 37 °C with 5% CO_2; 10 microliters of reagent from CCK8 assays were added to each well 48 h after incubation. The OD_{450} value was measured using a microplate reader

(TECAN Infinite 200 Pro, Switzerland) after 1 h of incubation at 37 °C. The experiments were performed in triplicate. The OD_{450} value in the presence of different concentrations of the compound was divided by the OD_{450} value of the negative control to calculate the percentage of cytotoxicity. Cytotoxicity curves were plotted using GraphPad Prism 5.0 (GraphPad Software Inc., San Diego, CA, USA).

The antiviral activities of Nova and remdesivir against SARS-CoV-2 were evaluated *in vitro*. Briefly, cells were seeded in 96-well plates at a density of 2×10^4 cells/well and grown for 24 h. Vero cells were infected at a multiplicity of infection (MOI) of 0.01 for 1 h at 37 °C. Virus was washed with DMEM twice and then cells were treated with a medium containing Nova at various concentrations or remdesivir at different concentrations (20 μmol/L, 4 μmol/L, 0.8 μmol/L, 0.16 μmol/L, 0.032 μmol/L) for 48 h. For the prophylactic administration test, Nova was added 2 h before viral infection and washed twice with DMEM. The cells were then incubated in fresh DMEM for 48 h. The supernatant was collected, and the RNA was extracted and analyzed by relative quantification by quantitative real-time reverse transcription polymerase chain reaction (qRT-PCR), as described in a previous study (*8*).

Viral RNA was extracted from 100 μL supernatant of infected cells using an automated nucleic acid extraction system (TIANLONG, Xi'an, China) following the manufacturer's recommendations. SARS-CoV-2 was detected using the One Step PrimeScript RT-PCR kit (TaKaRa, Shiga, Japan) on a LightCycler 480 Real-Time PCR system (Roche, Rotkreuz, Switzerland). ORF 1ab was amplified from cDNA, cloned into MS2-nCoV-ORF1ab, and used as the plasmid standard after its identity was confirmed by sequencing. A standard curve was generated by determining copy numbers from serial dilutions (10^3–10^9 copies) of the plasmid. The primers used for quantitative PCR were 1ab-F: 5'-AGAAGATTGG TTAGATGATGATAGT-3'; 1ab-R: 5'-TTCCATC TCTAATTGAGGTTGAACC-3', and probe 5'-FAM-TCCTCACTGCCGTCTTGTTGACCA-BHQ1-3'. The individual concentration for 50% of maximal effect (EC_{50}) values were calculated using GraphPad Prism 5.0. All experiments were conducted in triplicate.

RESULTS

Cell viability after Nova treatment was determined using the CCK8 assay in Vero cells. The 50% cytotoxic concentration (CC_{50}) of Nova was 1,076 ng/mL (Figure 1A). To investigate the antiviral effect of Nova against the ancestral SARS-CoV-2 virus, Vero cells were infected with the virus and incubated with Nova and remdesivir at various concentrations for 48 h. Remdesivir was selected as the positive control in our study, and the results showed that the EC_{50} of remdesivir was 1.52 μmol/L (Figure 1B). Nova inhibited the replication of the SARS-CoV-2 ancestral virus with an EC_{50} value of 0.0019 ng/mL (Figure 1C).

To illustrate the efficacy of Nova in inhibiting the SARS-CoV-2 Omicron variant replication *in vitro*, Vero cells were infected with the Omicron variant and incubated with Nova and remdesivir at various concentrations for 48 h. Results showed that remdesivir inhibited the Omicron variant with an EC_{50} of 0.75 μmol/L (Figure 1D). The EC_{50} values of Nova for SARS-CoV-2 Omicron variant were 0.0027 ng/mL (Figure 1E).

In Vero cells, pretreatment with different concentrations of Nova influences the replication of the SARS-CoV-2 Omicron variant. The EC_{50} of pretreatment with Nova for the SARS-CoV-2 Omicron variant was 0.2 ng/mL (Figure 1F). Taken together, these results indicated that pretreatment or treatment with type I IFN significantly inhibited both ancestral SARS-CoV-2 and Omicron variant infections *in vitro*.

DISCUSSION

Owing to the lack of specific antiviral drugs, rapid evaluation of the antiviral activity of existing licensed drugs is a critical method to combat the pandemic. Here, we showed that Nova inhibits replication of ancestral SARS-CoV-2 and the Omicron variant *in vitro*. Pretreatment with Nova protected cells against Omicron variant infection *in vitro*.

Type I IFNs are the first line of defense and are vital for blocking early viral replications, spread, and tropism, as well as promoting the adaptive immune response. Type I IFNs induce a systemic response that affects almost every cell in the host (*4*). It is reported that compared to the severe acute respiratory syndrome coronavirus, SARS-CoV-2 is more sensitive to IFN-I (*9*). In addition, IFN beta-1b was shown to decrease virus-induced lung fibrosis in a mouse model (*10*), which may improve the outcomes of patients with COVID-19 complicated by acute respiratory distress

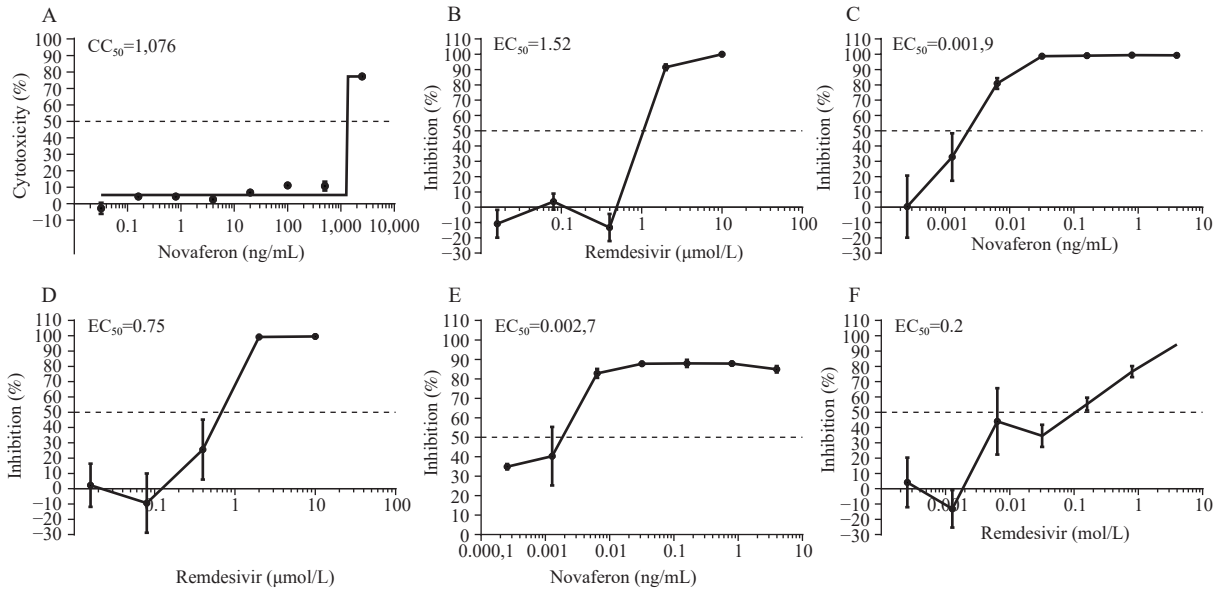

FIGURE 1. Cytotoxic effect of Nova and antiviral activities of Nova and remdesivir against ancestral SARS-CoV-2 and the Omicron variant in Vero cells.
(A) The cytotoxicity of Nova. (B and C) Antiviral activities of remdesivir and Nova against ancestral SARS-CoV-2. (D and E) Antiviral activities of remdesivir and Nova against the Omicron variant. (F) Prophylactic antiviral activity of Nova against the Omicron variant.
Abbreviations: Nova=Novaferon; SARS-CoV-2=severe acute respiratory syndrome coronavirus 2.

syndrome. These results were partly consistent with those of our previous study: Nova and Nova plus lopinavir/ritonavir groups had significantly higher viral clearance rates than the lopinavir/ritonavir alone or control groups (*7*).

As the SARS-CoV-2 Omicron variant replaced the Delta variant as the main pandemic virus in late 2021 in the world, the risk of severe breakthrough infection was high (*3*). Considering immune-compromised individuals and the high price of monoclonal antibody therapy and antiviral agents, more treatment options were urgently needed. The IFNs were proved to be safe and available, more clinical trials on IFNs alone or combined with other medicines were worth exploring.

However, there were limitations in this study. The inhibition of Nova against the ancestral SARS-CoV-2 and Omicron variant was only tested *in vitro*. The *in vivo* effects of Nova need to be tested in animal models such as K18-hACE2 mice. And more importantly, large-scale double-blinded clinical trials are needed to verify the efficacy of Nova in COVID-19.

In summary, we characterized the inhibition of Nova against ancestral SARS-CoV-2 infection *in vitro*. Antiviral activity of Nova was also observed in SARS-CoV-2 Omicron variant-infected cells. Furthermore, pretreatment of Vero cultures with Nova reduced SARS-CoV-2 replication. Overall, these data suggested that Nova is a potential candidate for the management of COVID-19 and could be worthy of further *in vivo* study and clinical trial.

Conflicts of interest: No conflicts of interest.

Funding: National Key R&D Program of China (2021YFC0863300).

doi: 10.46234/ccdcw2022.112

[#] Corresponding author: Wenjie Tan, tanwj@ivdc.chinacdc.cn.

[1] National Health Commission (NHC) Key Laboratory of Biosafety, National Institute for Viral Disease Control and Prevention, Chinese Center for Disease Control and Prevention, Beijing, China.

Submitted: April 07, 2022; Accepted: May 28, 2022

REFERENCES

1. Zhu N, Zhang DY, Wang WL, Li XW, Yang B, Song JD, et al. A novel coronavirus from patients with pneumonia in China, 2019. N Engl J Med 2020;382(8):727 – 33. http://dx.doi.org/10.1056/NEJMoa2001017.
2. World Health Organization. Coronavirus disease (COVID-2019) situation reports. https://wwwwhoint/emergencies/diseases/novelcoronavirus-2019/situation-reports. [2022-2-15].
3. Callaway E. Heavily mutated Omicron variant puts scientists on alert. Nature 2021;600(7887):21. http://dx.doi.org/10.1038/d41586-021-03552-w.
4. Lazear HM, Schoggins JW, Diamond MS. Shared and distinct functions of type I and type III interferons. Immunity 2019;50(4):907 – 23. http://dx.doi.org/10.1016/j.immuni.2019.03.025.
5. Mantlo E, Bukreyeva N, Maruyama J, Paessler S, Huang C. Antiviral activities of type I interferons to SARS-CoV-2 infection. Antiviral Res

2020;179:104811. http://dx.doi.org/10.1016/j.antiviral.2020.104811.
6. Li M, Rao CM, Pei DN, Wang L, Li YN, Gao K, et al. Novaferon, a novel recombinant protein produced by DNA-shuffling of IFN-α, shows antitumor effect *in vitro* and *in vivo*. Cancer Cell Int 2014;14:8. http://dx.doi.org/10.1186/1475-2867-14-8.
7. Zheng F, Zhou YW, Zhou ZG, Ye F, Huang BY, Huang YX, et al. SARS-CoV-2 clearance in COVID-19 patients with Novaferon treatment: a randomized, open-label, parallel-group trial. Int J Infect Dis 2020;99:84 – 91. http://dx.doi.org/10.1016/j.ijid.2020.07.053.
8. Yao XT, Ye F, Zhang M, Cui C, Huang BY, Niu PH, et al. In vitro antiviral activity and projection of optimized dosing design of hydroxychloroquine for the treatment of severe acute respiratory syndrome coronavirus 2 (SARS-CoV-2). Clin Infect Dis 2020;71(15):732 – 9. http://dx.doi.org/10.1093/cid/ciaa237.
9. Lokugamage KG, Hage A, De Vries M, Valero-Jimenez AM, Schindewolf C, Dittmann M, et al. Type I interferon susceptibility distinguishes SARS-CoV-2 from SARS-CoV. J Virol 2020;94 (23):e01410 – 20. http://dx.doi.org/10.1128/JVI.01410-20.
10. Luckhardt TR, Coomes SM, Trujillo G, Stoolman JS, Vannella KM, Bhan U, et al. TLR9-induced interferon β is associated with protection from gammaherpesvirus-induced exacerbation of lung fibrosis. Fibrogenesis Tissue Repair 2011;4:18. http://dx.doi.org/10.1186/1755-1536-4-18.

Indexed by PubMed Central (PMC), Emerging Sources Citation Index (ESCI), Scopus, Chinese Scientific and Technical Papers and Citations, and Chinese Science Citation Database (CSCD)

The inauguration of *China CDC Weekly* is in part supported by Project for Enhancing International Impact of China STM Journals Category D (PIIJ2-D-04-(2018)) of China Association for Science and Technology (CAST).

CCDC weekly

Vol. 4 No. 23 Jun. 10, 2022

Responsible Authority

National Health Commission of the People's Republic of China

Sponsor

Chinese Center for Disease Control and Prevention

Editing and Publishing

China CDC Weekly Editorial Office
No.155 Changbai Road, Changping District, Beijing, China
Tel: 86-10-63150501, 63150701
Email: weekly@chinacdc.cn

CSSN

ISSN 2096-7071
CN 10-1629/R1